Summary Sheet

- **Paper citation:**
  M. Eldessouki and M. Hassan, "Adaptive Neuro-Fuzzy System For Quantitative Evaluation of Woven Fabrics' Pilling Resistance," *Expert Systems with Applications,* vol. 42, no. 4, pp. 2098-2113, 2014, DOI:10.1016/j.eswa.2014.10.013.

- **Targeted problem:**
  Fabric pilling is measured according to ***subjective evaluation*** standards and while it is a ***surface property***, no research considered the ***textural features*** as descriptors and the classifications performed in the literature neglect the ***uncertainty*** during the ***decision making*** by the human operators

- **Objective(s):**
  - Develop an algorithm that considers the second-ordered statistical textural features of the fabric surface
  - Develop a method for creating a training dataset of a reasonable size suitable for the soft-computing classifier
  - Develop a classification system that counts for uncertainty in the decision making
  - Build an integrated system that combines these algorithms while being user-friendly

- **Materials scope:**
  - EMPA Standards (SN 198525) photographs were used as evaluation reference for training the artificial intelligence system
  - Fabrics produced with weaving technology of different structures and colors

- **Computation method:**
  - Second-order statistical and textural features as pills descriptors
  - Stochastic method for generating a dataset with a reasonable size
  - Adaptive neuro-fuzzy inference system (ANFIS) was used for the classification with some degree of uncertainity

- **Paper significance:**
  - Considered the *texture features* of the fabric images to quantize its pilling for the first time
  - Introduced a stochastic method for creating sampling dataset required in building the soft-computing classifier
  - Utilized the neuro-fuzzy classification system to approach the high level intelligence of human beings
  - Created a user-friendly GUI that integrates the main four stages of pilling evaluation

- **Software**
  A software program with a user-friendly GUI was developed for this paper. The software program for is included on the accompanied CD with a tutorial video demonstration. It also has example picture so the reader can test the program. The program's GUI is shown below:

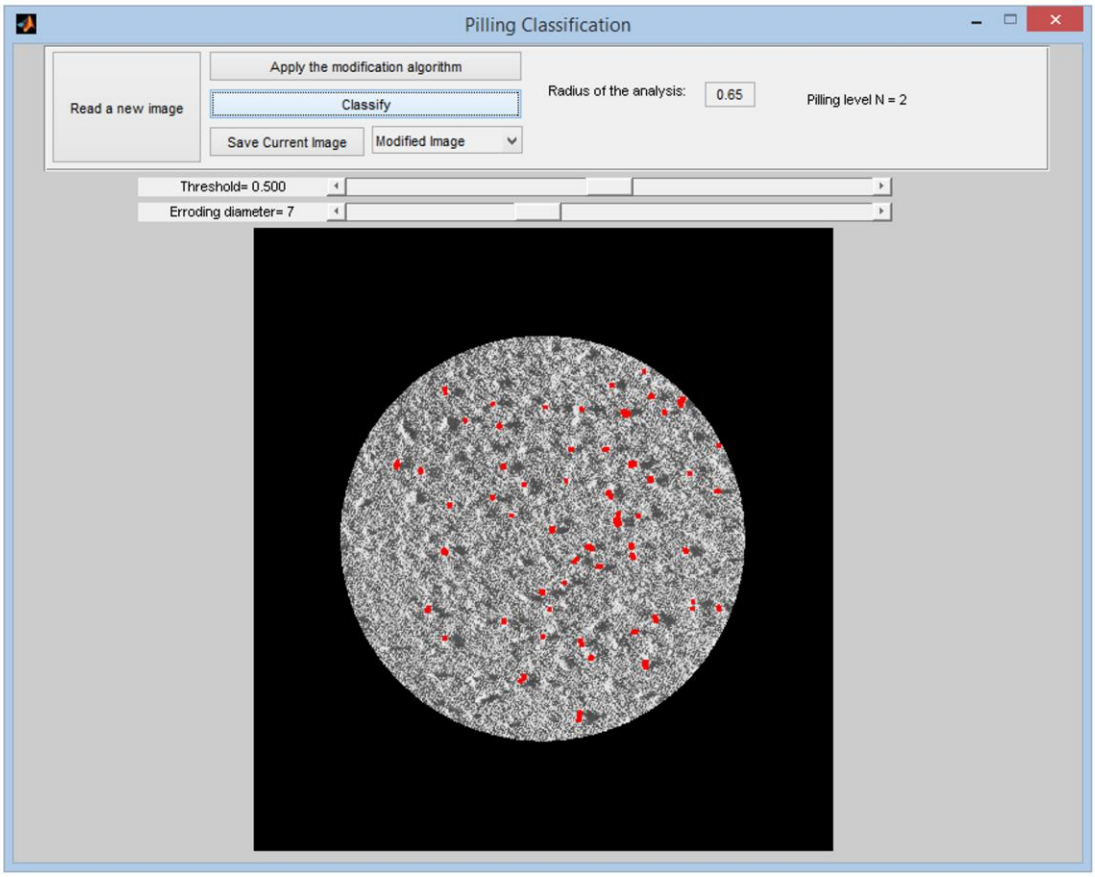
Pilling Classification
Read a new image
Apply the modification algorithm
Classify
Save Current Image
Modified Image
Radius of the analysis:
0.65
Pilling level N = 2
Threshold= 0.500
Erroding diameter= 7

Adaptive Neuro-Fuzzy System For Quantitative Evaluation of Woven Fabrics' Pilling Resistance

Mohamed Eldessouki[1,3*], Mounir Hassan[2,3]

[1] *Department of Materials Engineering, Technical University of Liberec, Czech Republic*

[2] *Faculty of Computing and Information Technology, King Abdulaziz University, Jeddah, Saudi Arabia*

[3] *Department of Textile Engineering, Faculty of Engineering, Mansoura University, Mansoura, Egypt*

* Corresponding author Email: eldesmo@auburn.edu

Abstract:

Fabric pilling is considered a performance and aesthetic property of the woven products that determine its quality. The subjective evaluation of the fabric pilling results in misleading values that depend on the measurement standard even for the same sample. This work utilizes some textural features extracted from the fabric's images to obtain better representative and quantitative values of the fabric's surface. An algorithm for creating features dataset for training and testing the soft-computing classifier was described where random noise was added to the limited number of fabric's pilling standard images. The objective pilling classification of the fabric samples was performed using an adaptive neuro-fuzzy system (ANFIS) which showed an ability to classify the noised standard images with a correct classification rate of 85.8%. The ANFIS was also able to classify actual fabric samples with a Spearman's coefficient of rank correlation at +0.985 when compared with the classification grades of the human operators. Results showed high efficiency of the system that is independent on the different fabric structure or color which suggests its availability to replace the currently applied subjective pilling evaluation.

1. Introduction

The quality control of the textile products is one of the major factors that determine the price, and therefore the profit, of these products. Among the important properties of fabrics are the *performance properties* which represent the response of the fabric to a certain force, exposure, or treatment. Performance properties of a fabric include the fabric strength, abrasion resistance, pilling, and color fastness. Fabric pilling is one of those properties that can be classified as performance or aesthetic properties of the fabric and, therefore, being critical phenomena for both the manufacturers and the consumers. According to the ASTM standard terminology related to textiles [1], pills can be defined as "bunches or balls of tangled fibers which are held to the surface of a fabric by one or more fibers". The fabric pilling is affected by a wide range of

parameters that may be related to: yarn parameters (e.g. twist, hairiness…etc), spinning technology (e.g. ring spinning, rotor, compact spinning…etc), fabric producing technology (e.g. weaving, knitting…etc), as well as other processing parameters [2].

Evaluating the fabric pilling during the quality control process depends in the majority of standard testing methods on accelerated fabric wear using laboratory devices that simulate the frictional mechanisms lead to surface wear and pilling formation. The available standards recommend comparing samples that gone under this accelerated wear process with standard photographs of different pilling grades where expert operators can judge the samples and assign a pilling grade to them. This results in a subjective evaluation of the fabric pilling with a great dependency on the human element. The majority of pilling standard evaluation methods assign a ranking system that ranges between 1 and 5 (where 1 is assigned to a sever pilling and 5 is assigned to no pilling). However, the existence of different standards (e.g. ASTM, SN, EN ISO,…etc) creates a lot of confusion as the same sample may be ranked with different pilling grades according to the standard that was used in the evaluation. This calls researchers for finding alternative objective evaluation methods that may help to standardize those standard methods [3].

Image analysis is a common technique in detecting textile faults [4] including their esthetic character as well as their irregularities [5]. The introduction of image analysis as a method for evaluating the fabric pilling started in the late 80's as a try to replace the applied subjective evaluation methods [6]. The application of the image processing and analysis in the evaluation of fabric pilling goes through four main stages as indicated in Figure 1 and the majority of the available literature on the topic tried to focus on one or more of these stages to modify the total outcome.

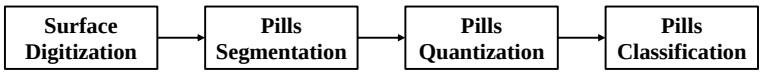

Figure 1. Stages of quantitative fabric pilling evaluation

The main four objective pilling evaluation stages can be explained as follow:

Fabric's surface digitization

The fabric surface digitization is the process of converting the fabric surface to a digital form that can be dealt with on computer systems. This process can be done using a digital scanner [7]–[11], a camera [3], [12]–[14], a light projected on camera [15], a camera attached to a microscope [16], optical triangulation topographic reconstruction of the fabric surface [17]–[19], a laser line

projected on the surface of the fabric specimen [20], or a stereovision surface reconstruction using two CCD cameras [20].

Pills detection and segmentation

Pills detection and segmentation is the process of separating the surface fuzz and pills from the complicated fabric structure background. This process was obtained using simple techniques such as the application of a binarization threshold on the fabric images [6], [20], or after processing the raw fabric images using spatial and spectral techniques. The raw image processing may include some filters for noise reduction or edge detection [10], a background dilation and erosion [13], [19], a fabric pattern detection and isolation using Fast Fourier Transform (FFT) [3], [11], [13], [14], [21] or the different techniques of wavelet transforms [8], [9], [21]–[24]. The pill detection was also performed using a template matching algorithm [14] and edge flow detection [25], [26]. For the colored images, pills were detected manually by blending the color channels of the fabric image [16].

Pills quantization

The pills quantization is the next stage after segmenting pills from the fabric image. The process focuses on extracting some features that numerically represent the pills population to allow a quantitative discrimination between the different images. The feature descriptors can be divided in two categories; one that depends on the final image of the segmented pills, and the second that utilizes the spectral decomposition and analysis that was performed during the pills segmentation. The first category of features includes simple features such as the number of pills, the total pixel area of pilling, mean area of pills, the relative area of the pills to the total surface area, the sum of the gray values of pill images, the total volume of pills, as well as the distributions of pills, their shape, orientation angle, contrast, and density or uniformity of pills spatial distribution on the fabric surface [3], [6], [7], [11], [13], [14], [16], [19], [20], [27]. The descriptor features can also be calculated from the gray-scale image of the processed surface or from the simulated fabric surface and includes roughness, skewness, as well as pills number, volume (total and average volumes), height (maximum and average), area (total and average), and fractal dimension [10], [15].

The second category of features includes the wavelet detail coefficients from the decomposition levels at the horizontal, the vertical and the diagonal orientations [24]. It can be defined also as the horizontal detailed coefficient (especially at scale close to the inter-yarn distances in the fabric) [9], as well as the energies of the reconstructed sub-images indifferent spatial orientations [22], [23]. Other statistical features can also be extracted from the wavelet decompositions such

as the range, the inter-quartile range, the variance, the standard deviation, the mean absolute deviation, the median absolute deviation, the standard error and the coefficient of variation [8].

Pills rating and classification

The classification stage is the ultimate goal of the whole process where a "successful" rating of images allows the trust in the method to replace the available subjective analysis. Classification models use the extracted set of features as inputs that can be used to generate the final rating of the image. The classification models may implement empirical and statistical methods such as the multi-variable linear regression [7], [14], [20] and discriminant analysis [8], [23], [24],or may implement artificial intelligent methods such as the application of different types of the artificial neural networks [15], [22], [28].

Based on this literature survey, three points can be highlighted:

- Although fabric wear and pilling are affecting the *texture* of the surface, there is no available publication that considers the image "textural parameters" during the pilling quantization.
- The classification methods based on artificial intelligence techniques require big databases for the system training and verification. However, the size of the dataset is limited because this dataset is based on photographs that are taken from standard images. Since the majority of standard methods utilize a rating system from 1 to 5, the standard images have a limited number that is not enough for creating a reasonable dataset size.
- There are few papers that consider the efficient techniques of each evaluation stage to create an integrated, robust, and effective evaluation process. On the other hand, the majority of these papers focus on enhancing one or more of these stages separately.

Therefore, this work tries to address these problems by:

- Considering the *texture features* of the images among the quantization parameters.
- Introducing a new method for creating sampling dataset that is large enough to suite the training and testing processes required in building the applied artificial intelligent classifier.
- Utilizing the neuro-fuzzy classification system to approach the high level of evaluation in human beings.

- Creating a user-friendly system that integrates the four evaluation stages. The system is semi-automatic in a way that classifies the pilling in the introduced sample automatically and allows the operator to change some of the detection parameters if not satisfied with the automatic detection.

2. Computation Theory:

2.1. Image preparation

The EMPA Standard (SN 198525) was used to obtain the standard images for pilling ranking. The EMPA standard has two series of photographs; the K-series for the knitted fabrics and the W-series for the woven fabrics. Among the W-series, there is the W1 category for evaluating the nonwoven fabrics while the W2 and W3 categories are used for evaluating the woven fabrics [3]. The W2 category is usually used in evaluating samples with big pill size while W3 is more suitable with samples of smaller pills. Within each category, there are four standard pictures used in the comparison and pills ranking on a scale of 1 (for the worst) to 5 (for the pill-free). To help the operators with their "fuzzy" and "subjective" evaluation, there are only four pictures for the five ranks where the first picture represents ranks 1-to-2, the second picture represents ranks 2-to-3,…etc. The standard photographs were scanned to the computer with a resolution of 600 x 600 dpi.

To generate a dataset with a suitable size out of these limited standard pictures, each standard image was duplicated many times where each copy had a random noise that was applied to it. To add noise to the pictures, different filter kernels were created with random parameters and each filter was convoluted with the picture to create a "noised" or "blurred" image. The applied filters are the "averaging", "disk", "Gaussian", "motion" filters, and the "partial spatial rearrangement". Representation of the original image and samples after the application of different noise filters are shown in Figure 2. The kernel for each filter was generated using random parameters that change each time of recalling the filter. The "partial spatial rearrangement" technique was applied by randomly selecting sub-image from the pilling region of the sample and having a size that represents 10% of the original image then placing the sub-image in a random way at a different position of the image.

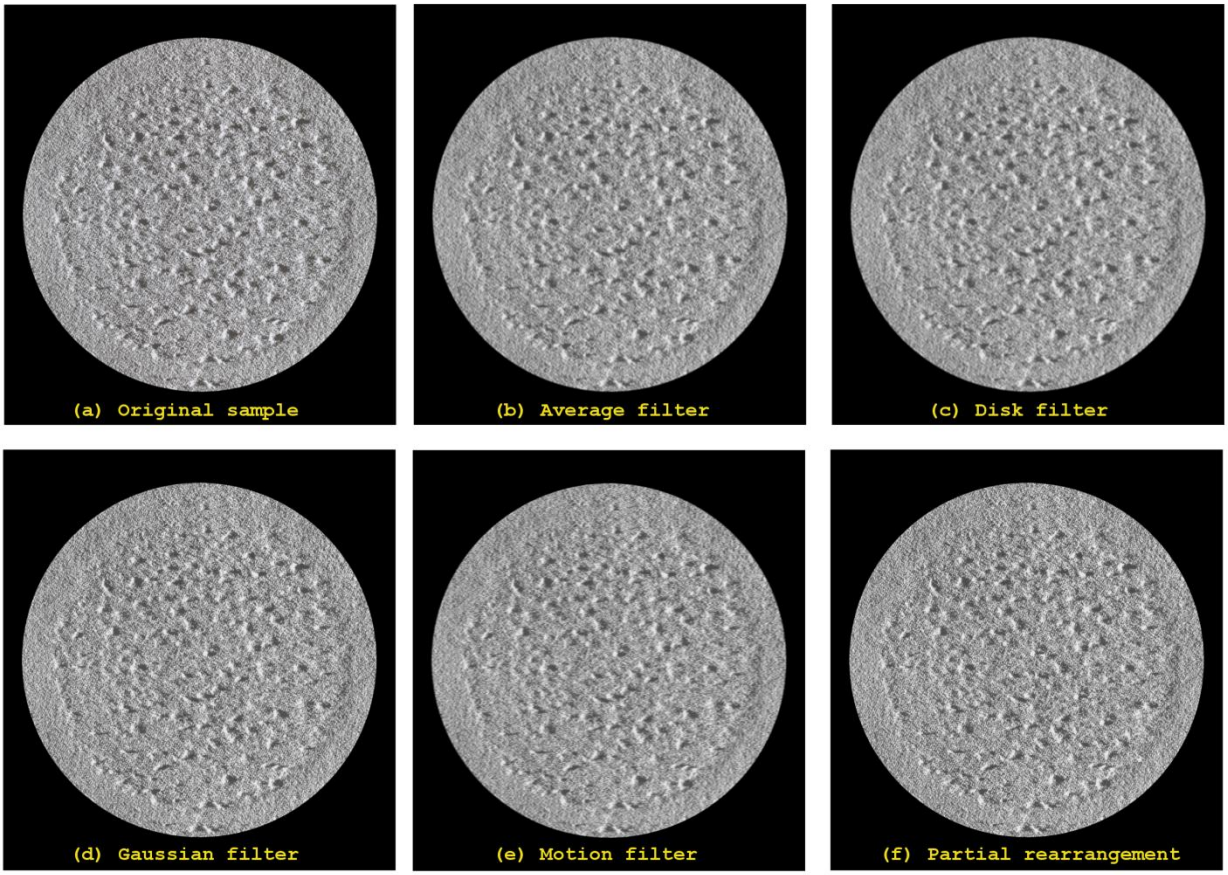

Figure 2. Examples for different shapes of the same fabric sample after applying random filters

These five types of noise generators were applied three times using random parameters to each standard picture which creates 15 noised copies of the original image. To avoid the system bias to the noised images, the features extracted from the original image were duplicated 35 times to create a features dataset with 30% representation of the noised images. The features dataset consists of the previously mentioned 4 features with 200 observations (50 observations for each standard image) of each standard category (W1, W2, and W3). The features dataset was then split randomly into a training dataset that represents 80% and a testing dataset that represents the remaining 20% of the data. The introduction of the noised images during the training of the classification system makes it more robust to classify different samples even with noised pictures.

2.2. Textural features

The basic statistics that are utilized in pilling quantization (the first order statistical features) extract data out of the gray-scale levels of the pixels in the digital image and does not reflect these surface features. On the other hand, the second order and textural features are more concerned about the spatial distribution of the gray-scale levels which reflects the roughness of the image and its texture. This gives the advantage of being close to the human awareness of the texture that describe surfaces as fine, coarse, smooth, rippled, irregular,...etc.

For an image with x and y representing the spatial coordinates, the gray-scale levels of that image can be expressed as $\boldsymbol{P}(x,y)$ and its gray level co-occurrence matrix (GLCM) can be calculated to determine the textural features of the image. The GLCM represents the joint probability density of the pairs of the gray levels occur at pairs of points separated by the vector $\boldsymbol{\delta}(\Delta x, \Delta y)$ [29]. The displacements Δx and Δy in the vector $\boldsymbol{\delta}$ determine the length (the running distance d) and the angel (direction θ) between the points of the required calculation. The calculated joint density takes the matrix form $\boldsymbol{C_\delta}$ with a size NxN where N is the maximum value of gray levels in the original image $\boldsymbol{P}$ and the value $\boldsymbol{C_\delta}(i,j)$ represents the probability of the pair of gray levels (i,j) occurring at separation $\boldsymbol{\delta}$. To illustrate the calculation of the GLCM, consider the example shown in Figure 3 for an image $\boldsymbol{P}(x,y)$ with N=4 gray levels values that range between 0 and 3. Therefore, the size of the co-occurrence matrix $\boldsymbol{C}$ is 4x4 and for a separation vector $\boldsymbol{\delta}(1,0)$ the entries $\boldsymbol{C_\delta}(i,j)$ are the number of times gray level i occur immediately (*i.e.* one pixel distance) to the left (*i.e.* in zero angel direction) of the gray level j.

Once the co-occurrence matrix was calculated the image texture can be analyzed based on the given parameters (d,θ) of the vector $\boldsymbol{\delta}$. If the image's texture is coarse and the displacement d is smaller than the size of the texture element, the pairs of points at separation $\boldsymbol{\delta}$ should have similar gray levels. Therefore, the high values in the co-occurrence matrix $\boldsymbol{C_\delta}$ should be concentrated at the main diagonal or its nearby. Similarly, for fine textured images with texture elements comparable in size to the separation $\boldsymbol{\delta}$, the values in $\boldsymbol{C_\delta}$ will be spread out. The same logic applies for the texture direction that might be directed to a certain angel and, therefore, the spread of the values about the main diagonal of $\boldsymbol{C_\delta}$ will depend on the selected angel (θ) of the vector $\boldsymbol{\delta}$. Therefore, an investigation of the image texture is required at different displacements (d) and directions (θ) then the scattering of values around the $\boldsymbol{C_\delta}$'s main diagonal should be measured.

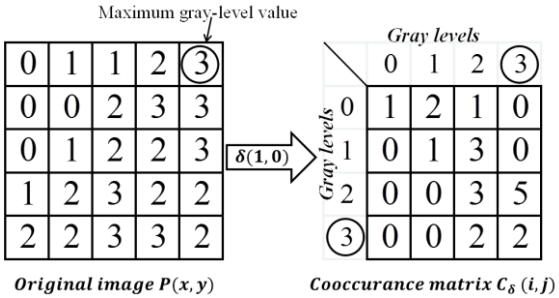

Figure 3. Demonstration for the construction of the GLCM for an image P(x,y)

To measure the spread of values in the co-occurrence matrix Haralick *et al* [30] suggested different features that represent the texture information of the image. The calculation of these features starts usually with the normalization of the matrix $\boldsymbol{C}$ by its total sum:

$$D_\delta(i,j) = \frac{C_\delta(i,j)}{\sum_{k=1}^{N}\sum_{l=1}^{N} C_\delta(k,l)}$$

Where *i*, *j*, *k*, and *l* are indices and $\boldsymbol{D_\delta}$ is the normalized matrix at a certain direction δ.

Among the features suggested by Haralick, four features were found to be more effective and will be tested in this study. These features are:

Contrast:

$$f_{1,\delta} = \sum_{i=1}^{N}\sum_{j=1}^{N}(i-j)^2 D_\delta(i,j)$$

The contrast is also known as the "*variance*", and the "*inertia*" and it is taken as a texture feature because it represents the moment of inertia of the matrix $\boldsymbol{D_\delta}$ around its main diagonal and it is a measure of the degree of its spread of values.

Correlation:

$$f_{2,\delta} = \sum_{i=1}^{N}\sum_{j=1}^{N}\frac{ijD_\delta(i,j) - \mu_i\mu_j}{\sigma_i\sigma_j}$$

Where μ_i, and σ_i are the mean and standard deviation, respectively, of the row sums and μ_j, and σ_j are the mean and standard deviation, respectively, of the column sums of the matrix $\boldsymbol{D_\delta}$. The correlation is a measure of the degree to which the rows (or columns) of the GLCM resemble each other and this value should be high when values are uniformly distributed in the matrix and low when the values off the diagonal are small.

Angular second moment (ASM):

$$f_{3,\delta} = \sum_{i=1}^{N}\sum_{j=1}^{N} D_\delta(i,j)^2$$

The angular second moment (ASM) is also known with different names such as the "*energy*", the "*uniformity*", and the "*uniformity of energy*". This value is small when $\boldsymbol{D_\delta(i,j)}$ are close in values and it increases when values largely varied as in the situation where values are clustered near the main diagonal.

Inverse difference moment (IDM):

$$f_{4,\delta} = \sum_{i=1}^{N}\sum_{j=1}^{N} \frac{D_\delta(i,j)}{1+(i-j)^2}$$

The inverse difference moment (IDM) can also be called the *homogeneity* and it measures the closeness of the distribution of elements in the GLCM to its diagonal and it reaches 1 for a diagonal matrix.

2.3. Adaptive Neuro-Fuzzy System

Fuzzy inference systems are useful in mapping data between two spaces while some degree of uncertainty is involved. The fuzzy system implements the membership functions, instead of the crisp-set functions, to imitate the human thinking and cognition without employing precise quantitative analyses [31]. This provides the opportunity to deal with imprecision and to represent the linguistic qualitative words such as "many", "low", "few"…etc. However, creating such fuzzy systems requires some understanding of the rules that govern the relations between the inputs and the outputs. Therefore, the adaptive neuro-fuzzy inference systems (ANFIS) were introduced to combine the natural language description of fuzzy systems and the learning properties of neural-networks. By using a hybrid learning algorithm, the ANFIS can construct an input-output mapping based on both human knowledge (in the form of fuzzy *if-then* rules) and stipulated input-output data pairs [31].

The initial model of the ANFIS was proposed by Jang [31], [32] who explained it using two inputs (x_1, x_2) and built the rule based system using two *if-then* rules, although the system can be generalized to any *N* number of inputs or *M* rules. The model with two inputs is demonstrated in Figure 4 with five layers that include two *adaptive* layers (layer #1 and layer #4, demonstrated by rectangles) and three *fixed* layers (layer #2, layer #3, and layer #5, demonstrated by circles). The two adaptive layers are distributed between the *premise* part, and the *consequent* part which

are the two basic components of all *logical statements*. The positioning of the adaptive layers at these two parts allows the adjustment of their parameters and consequently adjusting the performance of the whole system.

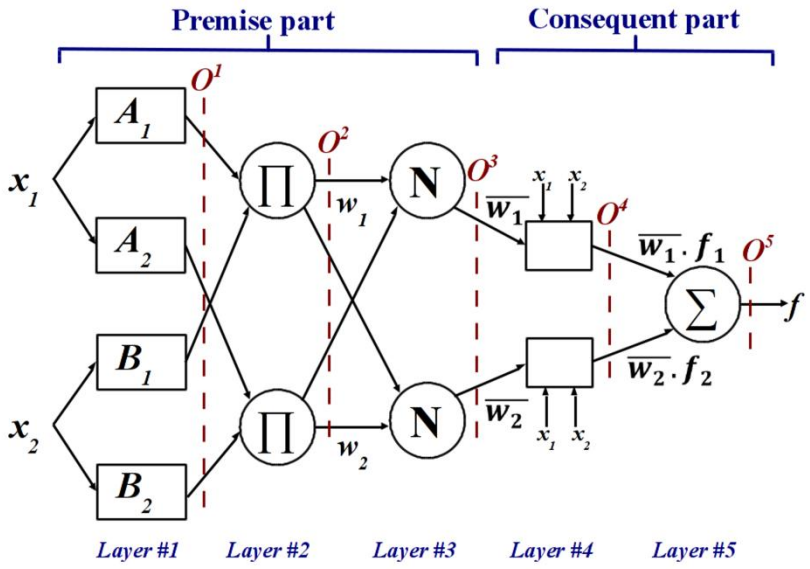

Figure 4. The ANFIS model

The two rules of Takagi and Sugeno were applied as:

Rule 1: If x_1 is A_1 and x_2 is B_1, then $f_1 = p_1x_1 + q_1 x_2 + r_1$

Rule 2: If x_1 is A_2 and x_2 is B_2, then $f_2 = p_2x_1 + q_2 x_2 + r_2$

The output of the k^{th} layer can be expressed with the vector O^k which can be stated for the first layer O^1 in the form:

$$O_i^1 = \begin{cases} \mu_{A_i}(x_1) \\ \mu_{B_i}(x_2) \end{cases}$$

Where μ_{A_i} and μ_{B_i} are the membership functions (MF) for the first and the second inputs, respectively. The membership function can take different shapes of any continuous and piecewise differentiable functions. The selected MF in this case is the Gaussian (bell shape) function with normalized output $\in [0,1]$ which can be written for the first input (x_1) in the following form (and a similar relation can be found for the second input):

$$\mu_{A_i}(x_1) = e^{-\left(\frac{x_1 - a_i}{b_i}\right)^2}$$

Where; the parameters {a_i and b_i} determine the shape and behavior of the membership function. These parameters will be called the *premise parameters* as they are the adjustable parameters in the premise part.

The neuron elements of the second layer are fixed with simple multiplication transfer function. The output of each neuron represents the *firing strength* of the rule. The output vector of this layer (O^2) can be calculated as:

$$O_i^2 = w_i = \mu_{A_i}(x_1).\mu_{B_i}(x_2)$$

The third layer is a fixed layer with the role of normalizing its inputs to produce the *normalized firing strength* which is the ratio of the firing strength of the i^{th} rule to the sum of the firing strength for all rules, that is:

$$O_i^3 = \overline{w_i} = \frac{w_i}{\sum_{j=1}^{N} w_j} = \frac{w_i}{w_1 + w_2}$$

Where, N is the number of the system inputs.

The fourth layer is the adaptive layer that multiplies the normalized firing strength by a first order polynomial for the first order Takagi and Sugeno model. The output vector of this layer O^4 can be expressed as:

$$O_i^4 = \overline{w_i} f_i = \overline{w_i}(p_i x_1 + q_i x_2 \ + \ r_i)$$

Where, the parameters {p_i, q_i, and r_i} are adjustable and can be used to tune the outputs of that layer. These parameters will be called the *consequent parameters* as they tune the output of the consequent part of the system.

The fifth layer has a single fixed neuron that sums up its inputs and produces the final result (f) of the system that can be represented as:

$$O_i^5 = f = \sum_{i=1}^{N} \overline{w_i} f_i = \frac{\sum_{i=1}^{N} w_i f_i}{\sum_{i=1}^{N} w_i}$$

2.4. Hybrid learning algorithm for the ANFIS

The goal of the learning of the ANFIS is to adjust all the tunable system parameters which includes both the premise parameters {a_i and b_i} and the consequent parameters {p_i, q_i, and r_i} to minimize the overall system's error. The hybrid learning algorithm utilizes two passes; the forward pass with fixed premise parameters and the backward pass with fixed consequent

parameters. To explain that, consider the forward pass with fixed premise parameters which results in an output that can be defined for the given two inputs ANFIS as:

$$f = \overline{w_1} f_1 + \overline{w_1} f_1 = \overline{w_1}(p_1 x_1 + q_1 x_2 + r_1) + \overline{w_2}(p_2 x_1 + q_2 x_2 + r_2)$$

That can be rearranged to:

$$f = (\overline{w_1} x_1) p_1 + (\overline{w_1} x_2) q_1 + (\overline{w_1}) r_1$$
$$+ (\overline{w_2} x_1) p_2 + (\overline{w_2} x_2) q_2 + (\overline{w_2}) r_2$$

It can be noticed from this equation that it represents a linear combination of the consequent parameters { p_1, q_1, r_1, p_2, q_2, and r_2 }. The least square method can be utilized to calculate those parameters. Therefore, the signal goes in the forward pass along the system until layer #4 then the least square method can be applied to allocate the consequent parameters and the whole system can be identified. The error rate of the system can be calculated after the system identification. The backward pass starts with fixing the consequent parameters and propagating the error rate backward through the system and the premise parameters {a_i and b_i} can be updated by the gradient descent method. This cycle continues until the desired performance is achieved as illustrated in Figure 5.

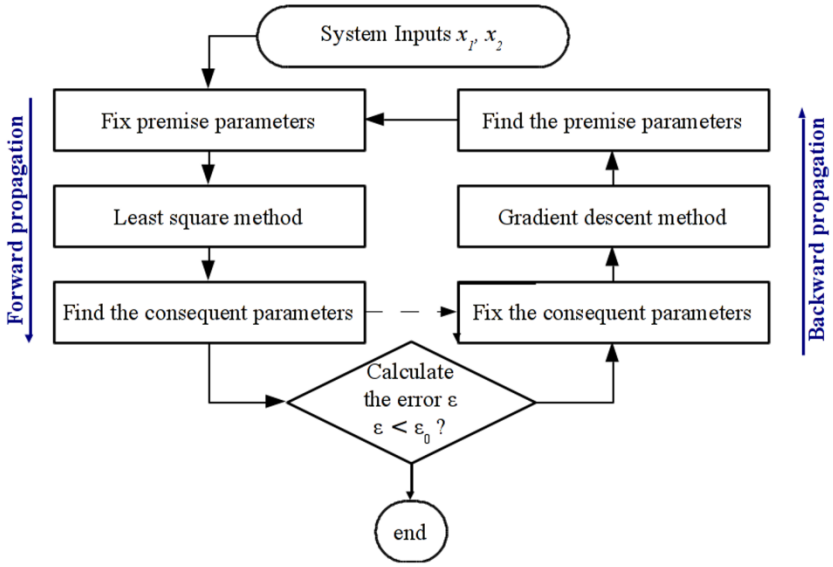

Figure 5. Hybrid ANFIS learning algorithm

3. Experimental Setup

Seven woven fabrics with different structures and colors are used and the specifications of these samples are listed in Table 1. To test the system ability in detecting the fabric pilling regardless

of the color shade, the tested samples were selected to have different colors. Samples were tested on Martindale instrument for pilling where two circular specimens of 140 mm diameters from each sample were placed on the machine head. The face of the lower specimen is up and the specimen is placed on the top of a standard felt of 140 mm diameter. The upper specimen is mounted on a holder of 90 mm diameter with a standard felt of the same size and fixed to the holder with an elastic ring. The upper holder is installed on the machine where the faces of the upper and lower specimens are in contact to each other. The samples were tested under 6.5 cN/cm^2 pressure for 10,000 cycles of Lissajous figure with 24 mm stroke.

Table 1. Tested knitted sample specifications

	Color	**Structure**	**Weight/Area (g/m^2)**	**Warp Density (threads/inch)**	**Weft Density (threads/inch)**	**Warp Count (tex)**	**Weft Count (tex)**
W1	White	1/6	128	71	70	21	21
W2	White	1/1	155	63	60	30	31
W3	Bright White	1/1	121	81	51	19	26
W4	Blue	1/3	145	86	56	21	32
W5	Blue	2/4	157	87	64	22	29
W6	Light Blue	1/3	167	88	55	21	38
W7	Paige	1/2	182	89	79	24	25

The measured samples were evaluated visually by seven different operators against the photographs of the EMPA Standards (SN 198525). The measured samples were then digitized using the setup shown in Figure 6 and processed using the developed software algorithm to obtain the pilling classes. The image acquisition system consists of a digital CCD camera that is equipped with a macro lenses to capture the sample surface details. The captured image resolution of 300 dpi and the image dimensions was 2048x1536 pixels. Lighting is critical for the imaging system and two light sources that equally distribute the light on the surface of the fabric were applied. The sample was tilted with a slight angel to the horizontal plane to allow contrasting the pills with their shadow.

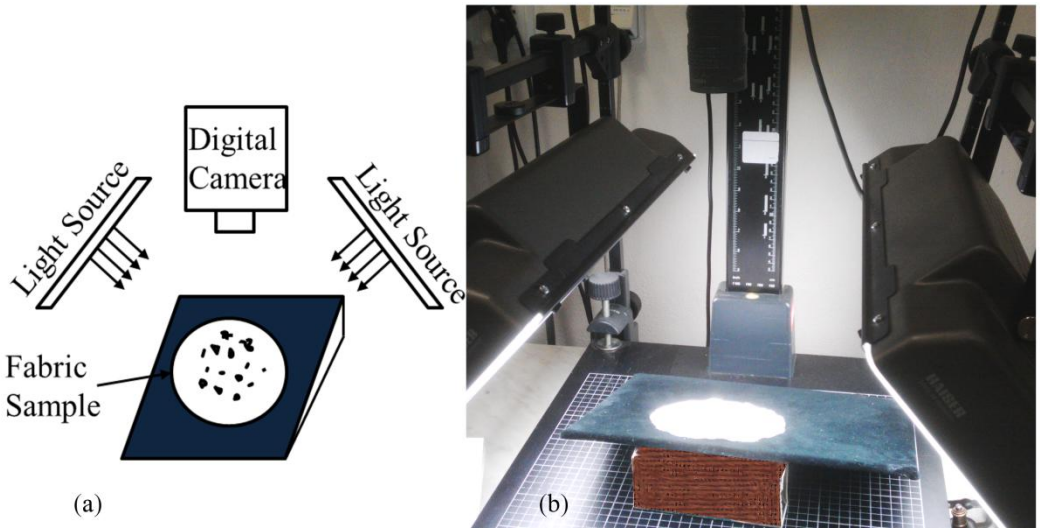

Figure 6. Image acquisition setup depicted schematically in (a) and photographed in (b)

4. Results and discussion:

Pre-investigation for the effective choice of the vector δ was performed by applying a distance sweep in the range of d = 0 to 50 with a step of one pixel. For long range investigations, another distance sweep in the range of 5 to 200 with a step of 5 pixels was also performed. In each case of the evaluation (the short term and the long term), a direction sweep was performed at four angles θ = 0°, 45°, 90°, and 135°. Results of the four extracted features for the short and long term distance sweeps are shown in Figure 7 to Figure 14 for the first sample of each standard category (i.e. W1_1-2, W2_1-2, and W3_1-2).

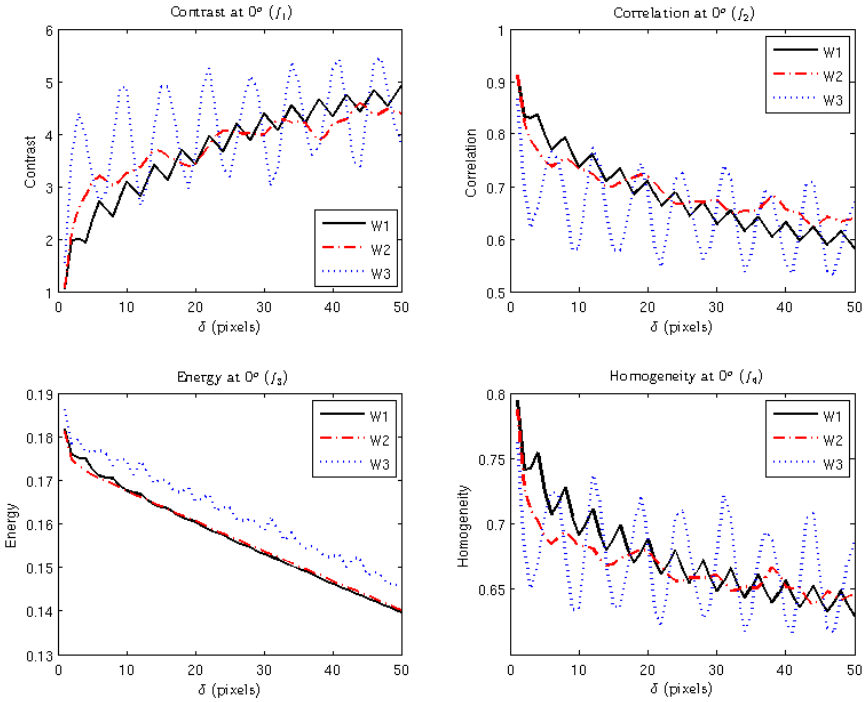

Figure 7. Features of the three categories at an angle of 0˚ and short term distance

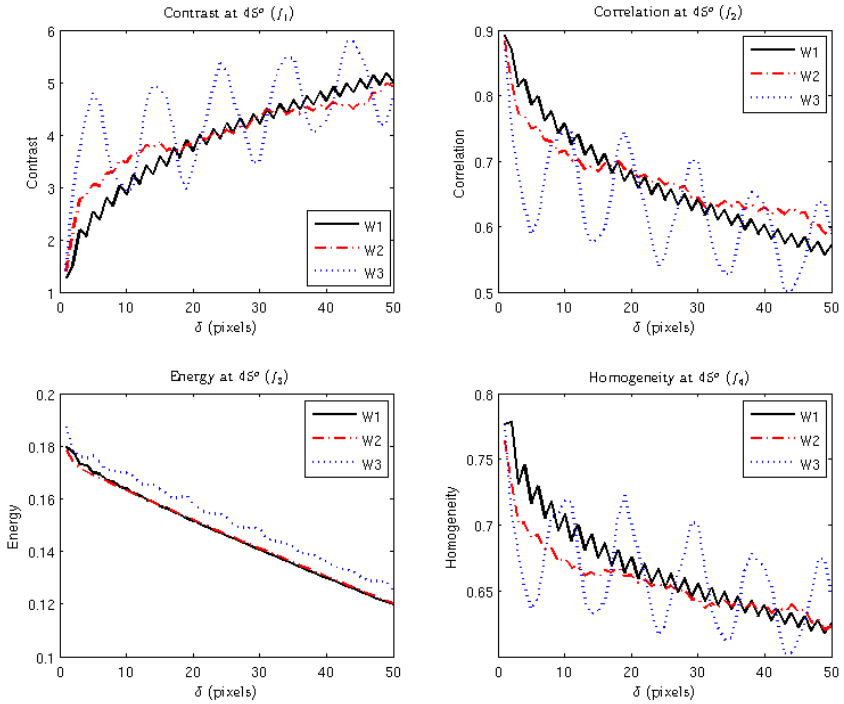

Figure 8. Features of the three categories at an angle of 45˚ and short term distance

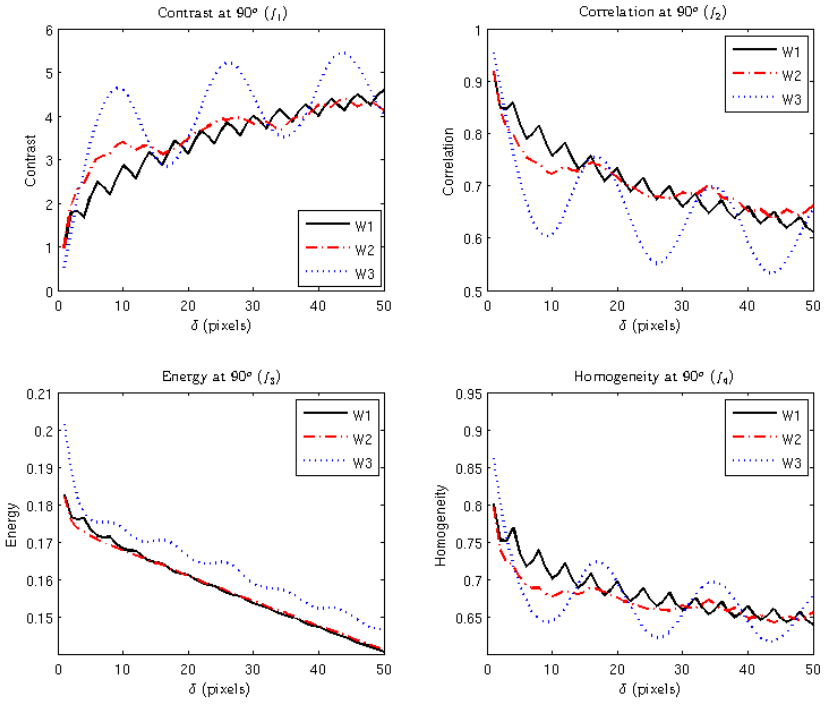

Figure 9. Features of the three categories at an angle of 90˚ and short term distance

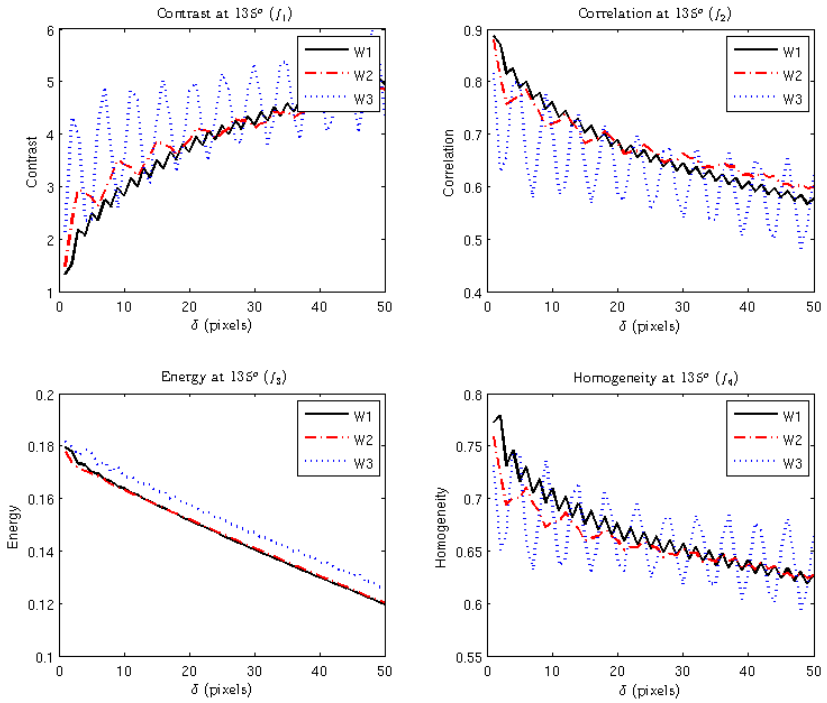

Figure 10. Features of the three categories at an angle of 135˚ and short term distance

Table 2. Features periodicity at short distance (values in pixels)

		f_1	f_2	f_3	f_4
Zero	W1	4	4	-	4
	W2	9*	-	-	9
	W3	6.5	6.5	-	6
45°	W1	4	4	-	4
	W2	9	9	-	9*
	W3	6	6	-	6
90°	W1	4	4	-	4
	W2	15	15*	-	9*
	W3	17	17	-	17
135°	W1	2	2	-	2
	W2	6.5	6.5	-	7
	W3	5	5	-	5

* Low correlation was observed at these values

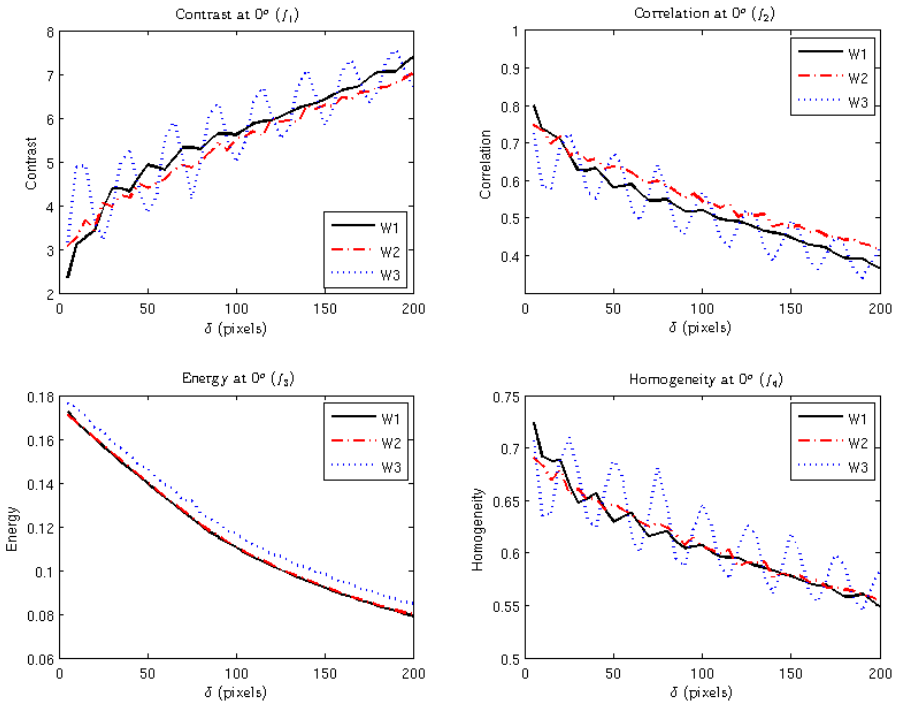

Figure 11. Features of the three categories at an angle of 0° and long term distance

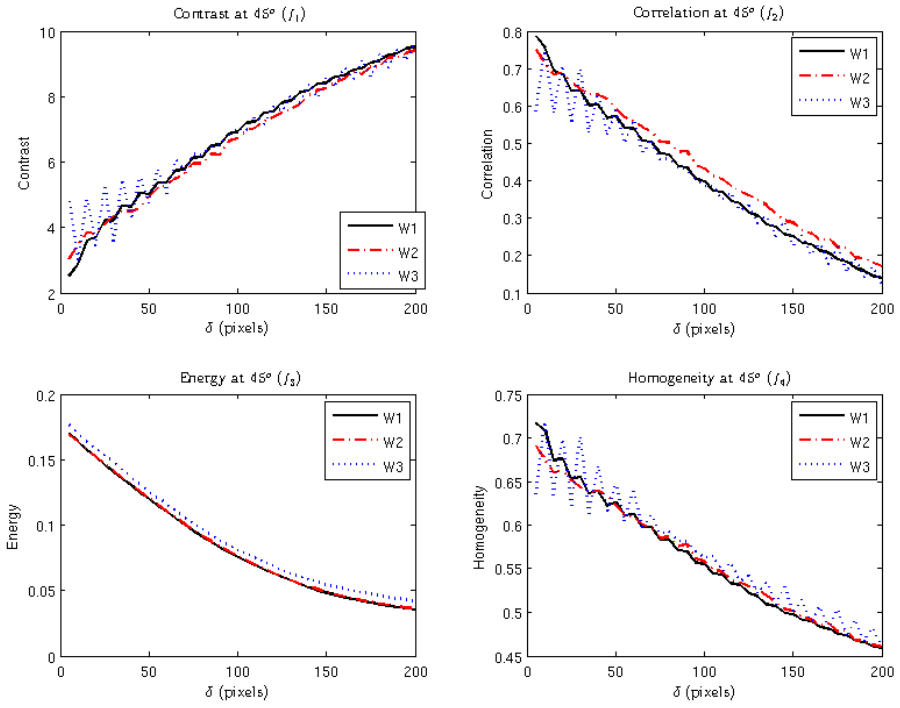

Figure 12. Features of the three categories at an angle of 45˚ and short term distance

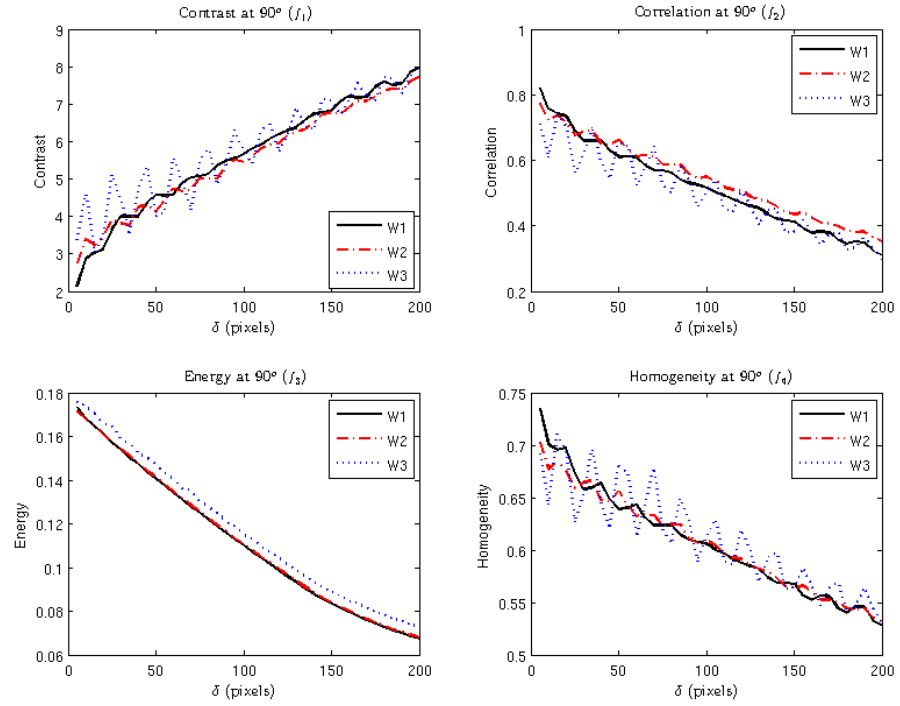

Figure 13. Features of the three categories at an angle of 90˚ and short term distance

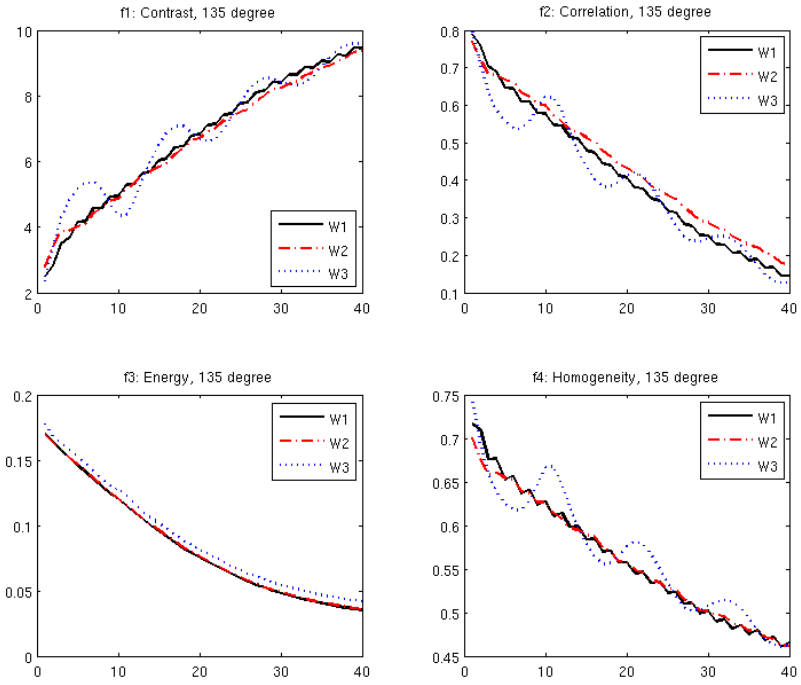

Figure 14. Features of the three categories at an angle of 135˚ and short term distance

Table 3. Features periodicity at long distance (values in pixels)

		f_1	f_2	f_3	f_4
Zero	W1	20	20	-	20
	W2	10	10	-	10
	W3	25	25	-	25
45˚	W1	-	10	-	10
	W2	-	25	-	25
	W3	10	10	-	10
90˚	W1	20	20	-	20
	W2	15	15	-	15
	W3	20	20	-	20
135˚	W1	10	10	-	10
	W2	-	-	-	-
	W3	55	55	-	55

From these figures some general notes can be observed on the fabric surface and its textural features:

- The behavior of the contrast feature (f_1) increases with increasing the calculation distance (δ) which is different from the other three features that decrease with distance.
- There is a form of periodicity in the behavior of most features, although this periodicity is not dominant in the energy feature (f_3) compared to the other features.
- The periodicity of the features can be considered as an indicator of the repeatability of objects on the fabric's surface at a certain distance. For example, by examining features f_1, f_2, f_4 at an angle of zero in Figure 7, a cyclic pattern can be observed with repeats of 4 pixels in category W1, 9 pixels in category W2, and 6 pixels in category W3. This indicates a repeatability of objects at these distances which might imply the repeatable pattern of the woven structure.
- The periodicity of features shown in Figure 7 to Figure 10 at short distances is summarized in Table 2 while the periodicity of the long distances shown in Figure 11 to Figure 14 is summarized in Table 3. Some features show periodicity although it might not be strong in some cases which were highlighted in the table with “low” and with the periodic interval, when available.
- Periodicity interval is almost constant when obtained from different features for the same fabric image.
- There is a small effect of the calculation angle on the periodicity of the features where similar intervals can be observed at different angles. The cases where a difference can be observed for the feature at different angles (e.g. f_1 at the angles 0° and 90°) might be attributed to the different warp and weft densities in the image.
- The repeat for a feature as observed at long distances is a multiplier of the repeat value for the same feature at short distance. For example the repeat of f_1 at 0° for W1 is 4 pixels (Table 2) while this value is 20 pixels (Table 3) when measured at long distance. This can be attributed to the different step size of evaluation during the short distance (1 pixel) and the long distance (5 pixels).
- Features that repeat at short distances were found to diminish after certain distance. For instance, the feature f_1 at 45° for W3 is found to have a strong repeating wave as observed in Figure 8 while this wave diminishes at long distances as shown in Figure 12. This

indicates the lack of correlation between the textural objects on the fabric's surface at long distances.

On the other hand, the change of the features at different directions at short distances is shown in Figure 15. There is a high similarity of the features' general trend at different angles with a coincidence allocation of the peaks at certain distances. The strength of the repeatable peak is decaying with distance and there is no significant repeatable behavior observed at longer distances (up to 200 pixels). The frequency of the peaks at 90° is almost double the frequency at 0° while a similar high frequency can be found at the angles 45° and 135°.

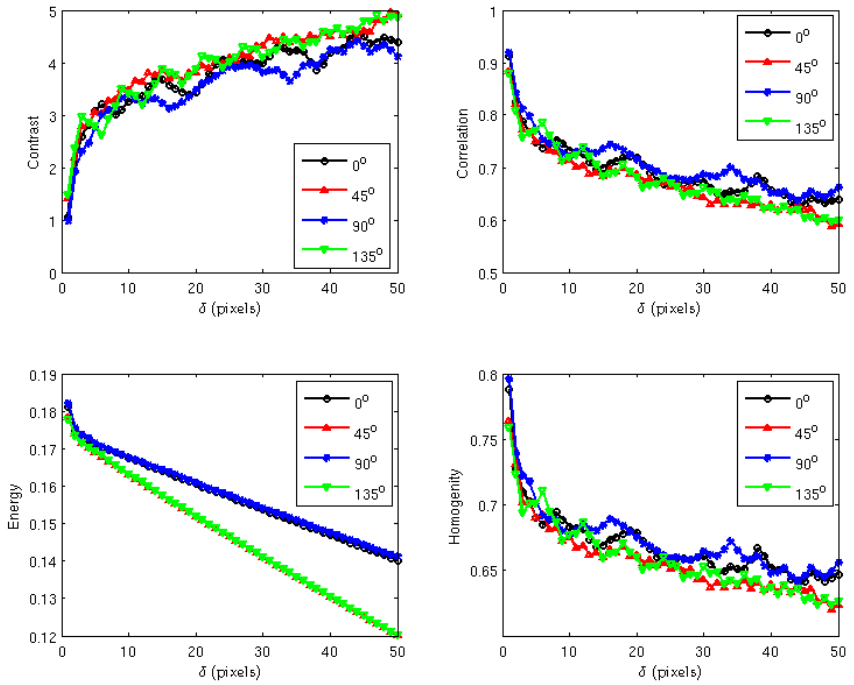

Figure 15. Features as calculated at different angles for sample W2_1-2

According to this pre-investigation, the actual samples are evaluated at an angle of 45° which should be a reasonable step that will coincide with angles of 0°, 90°, and 135° as indicated in the previously discussed figure. Features are also evaluated at a range of distance that covers the periods of peak maxima of the different features of the three categories. Based on the repeatability values listed in Table 2, the features are calculated in the distance interval from 4 to 10 pixels then values are summed up to be used as the characteristic features of the image during its evaluation. Also, due to the behavior similarity for the features, only the contrast and the correlation are used during the evaluation. These features are selected because they have a repeatable behavior and opposite trends. The other two features for evaluating the fabric pilling will be the number of pills and their relative area which is calculated as ratio between the pills area and the total area of interest in the studied sample.

Based on the described algorithm, an adaptive neruo-fuzzy system was constructed as shown in Figure 16 where the first adaptive layer consists of 3 neurons (3 membership functions) for each input. The premise parameters of this layer were calculated and the adjusted membership functions for the four inputs are shown in Figure 17. The multiplication and normalization were performed in the rule layer which is highlighted in Figure 16 with the blue color. The second adaptive layer is also shown in the same figure where the Takagi and Sugeno model applies and the consequent parameters are evaluated.

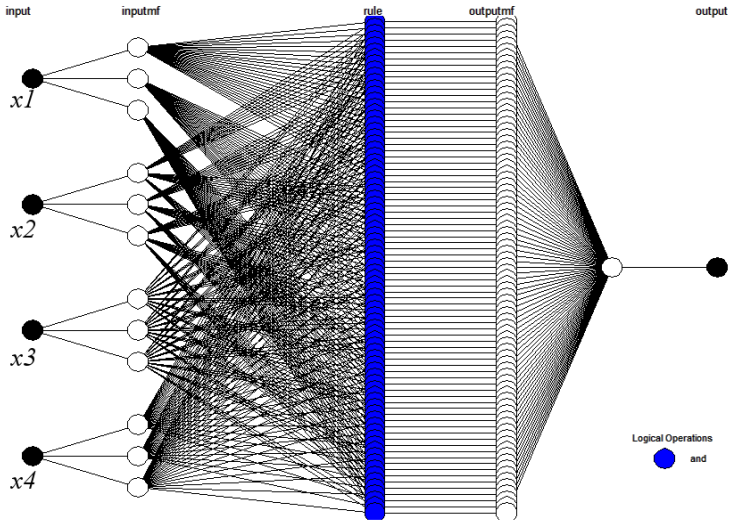

Figure 16. The ANFIS architecture for the given four inputs

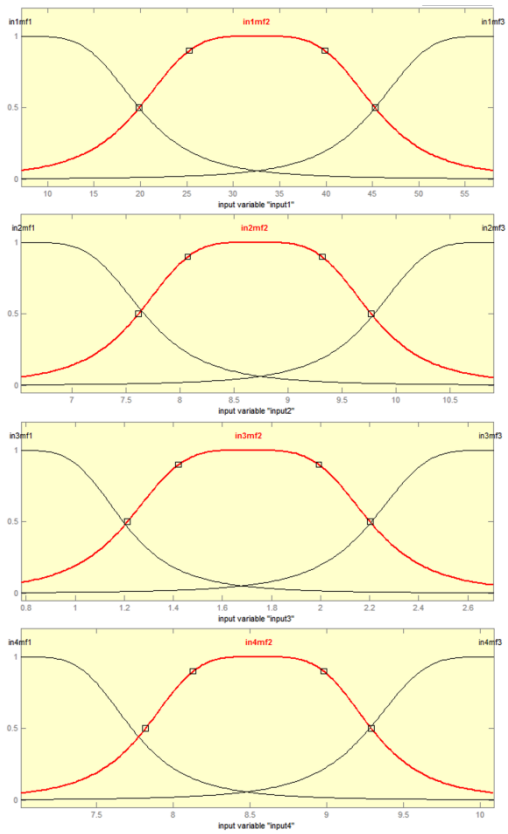

Figure 17. The adjusted membership functions for the four inputs (each input has two MFs)

The application of the ANFIS system is demonstrated in Figure 18 which includes the five basic steps of the calculation. The system starts with the *fuzzification* of the inputs where each input is processed in parallel through the membership functions. Second, the rules are applied using the *fuzzy operator* (AND) which results in the weighted firing strength to the third part of the *implication* and transfers data from the premise to the consequent. The fourth step is defined by the *aggregation* of the consequents across the rules and the final step is the *defuzzification* of the results to produce the final output.

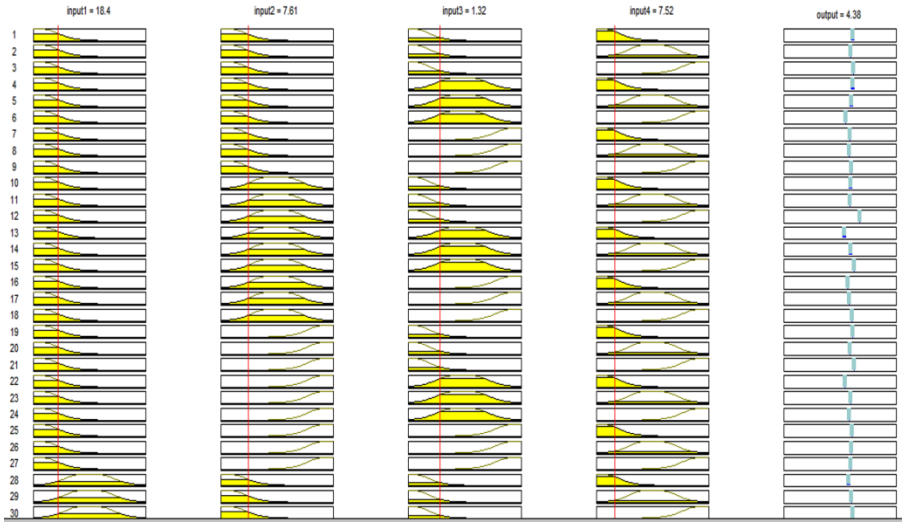

Figure 18. The application of the ANFIS

The given ANFIS structure was trained with the contrast, correlation, number of pills, and their relative areas as inputs and the standard pilling grades or ranks (1, 2, 3, 4 or 5) as outputs. The performance of the ANFIS systems is shown in Figure 19. For the 120 samples presented to the ANFIS systems, it can be seen that the ANFIS performed 85.8% in determining the pilling grade. Also, from these figures it can be observed that most of the samples that were miss-graded were deviated from the target class with only one degree which is acceptable in classifying such samples where the standards give two grades in the same picture.

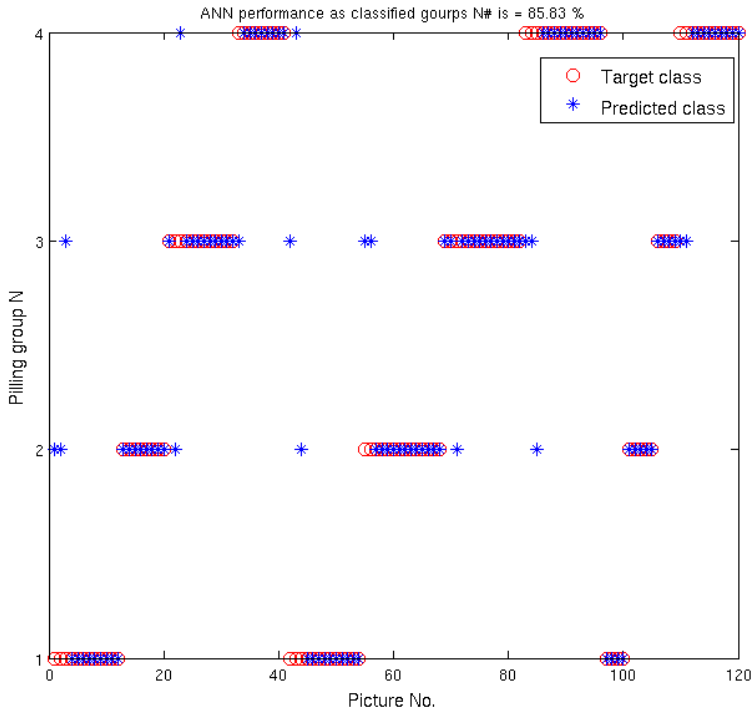

Figure 19. Performance of the ANFIS for the Nth grade

Although the relatively high performance of the ANFIS in detecting the correct pilling of the noised standard images, it is important to test the system on real fabric samples. Therefore, the developed algorithm was coded in a user-friendly graphical user interface (GUI) that is shown in Figure 20. The woven samples were introduced to seven human operators after their pilling test on Martindale to compare the samples with the standard pictures. The operators subjectively assigned a pilling rank for each sample as shown in Table 4 and the total pilling evaluation of the sample was calculated by the mode of the operator's ranks. The pictures of the woven samples were also introduced to the developed program that utilizes the ANFIS to rank the samples. The samples' pilling rank is listed in Table 4 and the Spearman's coefficient of rank correlation between the two categories of the human evaluation and the ANFIS evaluation is +0.982 which implies a good agreement between the two sets of results and a reliability of the system to be used in replacing the subjective evaluation of human operators.

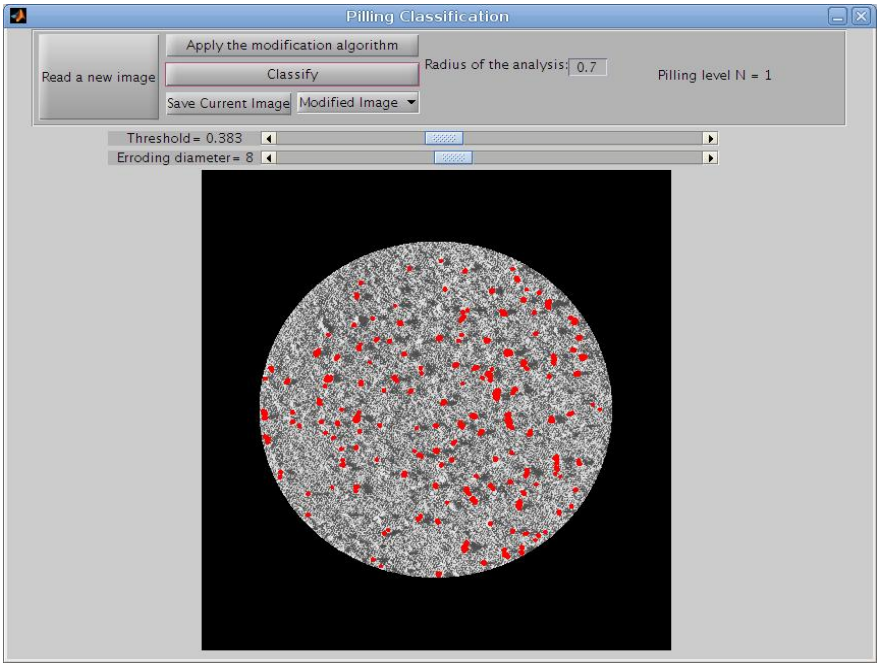

Figure 20. GUI of the developed software for fabric's pilling evaluation

Table 4. Human operators as compared to the ANFIS pilling evaluation

	OP.#1	OP.#2	OP.#3	OP.#4	OP.#5	OP.#6	OP.#7	Operators' evaluation	ANFIS evaluation
W1	3	3	1	2	2	2	2	2	2
W2	4	4	4	4	4	3	4	4	4
W3	3	2	2	1	4	2	2	2	2
W4	2	3	2	3	3	1	2	2	3
W5	2	1	1	1	3	2	1	1	1
W6	4	5	4	4	4	5	4	4	4
W7	3	3	3	3	4	2	5	3	3

Conclusion

This work introduces for the first time, to the best of the authors' knowledge, fabric's *image textural features* as measures for the fabric surface during the quantitative evaluation of pilling in woven fabrics. Creating a feature dataset from the available Standard images with enough size for training soft computing algorithms is challenging due to the limited number of those Standard images. To deal with this issue, a new approach was suggested to mimic the noise that interferes with the fabric surface during its digitization. Hence, a user-friendly pilling evaluation system

that integrates the processes of fabric surface digitization, pilling segmentation, quantization, and classification was implemented in this work. The system was able to classify woven fabric samples according to their surface texture with a high degree of correlation to the traditional methods of pilling evaluation.

Results of textural features show a trend similarity between the features which allows the reduction of the number of these features during the evaluation (contrast and correlation were only used in the final code). Selection of few features was not only to prevent redundancy in the system's inputs, but also to allow other pilling descriptors (such as the number of pills and their relative area) that represent pilling intensity to be considered. Taking more pilling descriptors into account during the pilling quantization might be useful; however the computational resources required for the ANFIS classifier increases exponentially with the increase in number of the system's inputs. This applies a constraint on the number of pilling descriptors that can be simultaneously used during the ANFIS classification which results in a "features optimization problem" due to the need of features that represent both the image texture as well as the pilling intensity quantifiers. A major part of the figures in the results section presented in this work was dedicated to investigate the texture features at different conditions and optimize their selection.

The application of random noise filters on the Standard images significantly affects the textural features while keeping a small effect on the pilling intensity features. The parameters of the applied filters were randomly selected; however the range of these parameters should extend to apply more "aggressive" noise to the pictures to allow the robustness of the system to deal with fabric images of different structures and textures. Also, more noise filters might be required to better resemble the image defects that might occur during the image acquisition, although the current filters were useful in increasing the amount of sampling datasets.

Success in digitizing the Standard samples in the same systematic fashion of real samples (rather than scanning Standard images) should increase the reliability of the suggested system and allows it to be standardized as a quantitative method that replaces the current subjective evaluation Standards. The relatively good results of the suggested system are promising for the methodology extension to cover fabrics that are produced using different technologies (knitted and nonwoven fabrics) as well as fabrics of different structures.

References

[1] D. Committee, "ASTM D123 - 13a Standard Terminology Relating to Textiles," *ASTM*. 2003.

[2] S. L. Paek, "Pilling, Abrasion, and Tensile Properties of Fabrics from Open-End and Ring Spun Yarns 1," *Text. Res. J.*, vol. 59, no. 10, pp. 577–583, 1989.

[3] B. K. Behera and T. E. M. Mohan, "Objective measurement of pilling by image processing technique," *Int. J. Cloth. Sci. Technol.*, vol. 17, no. 5, pp. 279–291, 2005.

[4] M. Eldessouki, M. Hassan, K. Qashqary, and E. Shady, "The Application of Principal Component Analysis to Boost The Performance of The Automated Fabric Fault Detector And Classifier," *FIBRES Text. East. Eur.*, vol. 22, no. 4(106), pp. 51–57, 2014.

[5] M. Eldessouki, S. Ibrahim, and J. Militky, "A Dynamic and Robust Image Processing Based Method for Measuring Yarn Diameter and Its Variation," *Text. Res. J.*, vol. 84, no. 18, pp. 1948–1960, 2014.

[6] A. Konda, L. C. Xin, Y. Okoshi, and K. Toriumi, "Evaluation of Pilling by Means of Computer Image Analysis Part 2 : Evaluation of Pilling Classes," *Sen'i Kikai Gakkaishi (Journal Text. Mach. Soc. Japan)*, vol. 41, no. 11, pp. T152–T161, 1988.

[7] S. C. Kim and T. J. Kang, "Image analysis of standard pilling photographs using wavelet reconstruction," *Text. Res. J.*, vol. 75, no. 12, pp. 801–811, 2005.

[8] S. R. Palmer, I. Joud, and X. Wang, "Characterization and application of objective pilling classification to patterned fabrics," *J. Text. Inst.*, vol. 96, no. 6, pp. 423–430, 2005.

[9] S. Palmer and X. Wang, "Objective classification of fabric pilling based on the two-dimensional discrete wavelet transform," *Text. Res. J.*, vol. 73, no. 8, pp. 713–720, 2003.

[10] D. Semnani and H. Ghayoor, "Detecting and measuring fabric pills using digital image analysis," *World Acad. Sci. Eng. Technol.*, vol. 49, pp. 897–900, 2009.

[11] S. Y. Yun, S. Kim, and C. K. Park, "Development of an objective fabric pilling evaluation method. I. Characterization of pilling using image analysis," *Fibers Polym.*, vol. 14, no. 5, pp. 832–837, 2013.

[12] C. H. Hsi, R. R. Bresee, and P. A. Annis, "Characterizing fabric pilling by using image-analysis techniques. Part I: Pill detection and description," *J. Text. Inst.*, vol. 89, no. 1, pp. 80–95, 1998.

[13] Y. Torres and R. Navarro, "Automatic method based on image analysis for pilling evaluation in fabrics," *Opt. Eng.*, vol. 37, no. 11, pp. 2937–2947, 1998.

[14] B. Xin, J. Hu, and H. Yan, "Objective evaluation of fabric pilling using image analysis techniques," *Text. Res. J.*, vol. 72, no. 12, pp. 1057–1064, 2002.

[15] X. Chen and X. B. Huang, "Evaluating fabric pilling with light-projected image analysis," *Text. Res. J.*, vol. 74, no. 11, pp. 977–981, 2004.

[16] J. Izabela, "Assessment of a Fabric Surface after the Pilling Process Based on Image Analysis," *Fibres Text. East. Eur.*, vol. 17, no. 2, p. 73, 2009.

[17] A. de Oliveira Mendes, P. T. Fiadeiro, and R. A. L. Miguel, "Subjective and objective pilling evaluations of textile fabrics: a comparison," *Text. Res. J.*, vol. 80, no. 18, pp. 1887–1897, 2010.

[18] A. de Oliveira Mendes, P. T. Fiadeiro, and R. A. L. Miguel, "Virtual subjective pilling evaluation: an alternative," *Text. Res. J.*, vol. 81, no. 9, pp. 892–901, 2011.

[19] A. de Oliveira Mendes, P. T. Fiadeiro, R. A. L. Miguel, and J. M. Lucas, "Optical estimation of a set of pilling coefficients for textile fabrics," *Text. Res. J.*, vol. 79, no. 5, pp. 410–417, 2009.

[20] T. J. Kang, D. H. Cho, and S. M. Kim, "Objective evaluation of fabric pilling using stereovision," *Text. Res. J.*, vol. 74, no. 11, pp. 1013–1017, 2004.

[21] S. Palmer, J. Zhang, and X. Wang, "New methods for objective evaluation of fabric pilling by frequency domain image processing," *Res. J. Text. Appar.*, vol. 13, no. 1, pp. 11–23, 2009.

[22] J. Zhang, X. Wang, and S. Palmer, "Objective pilling evaluation of nonwoven fabrics," *Fibers Polym.*, vol. 11, no. 1, pp. 115–120, 2010.

[23] J. Zhang, X. Wang, and S. Palmer, "Objective pilling evaluation of wool fabrics," *Text. Res. J.*, vol. 77, no. 12, pp. 929–936, 2007.

[24] J. Zhang, X. Wang, and S. Palmer, "Objective grading of fabric pilling with wavelet texture analysis," *Text. Res. J.*, vol. 77, no. 11, pp. 871–879, 2007.

[25] Z.-T. Xiao and H.-W. Yang, "Fabric Pilling Segmentation Based on Edgeflow Algorithm," in *Machine Learning and Cybernetics, 2007 International Conference on*, 2007, vol. 3, pp. 1744–1748.

[26] L. Xiaojun, "Segmentation for Fabric Pilling Images Based on Edge Flow," in *Information and Computing Science, 2009. ICIC'09. Second International Conference on*, 2009, vol. 2, pp. 369–372.

[27] C. H. Hsi, R. R. Bresee, and P. A. Annis, "Characterizing Fabric Pilling by Using Image-analysis Techniques. Part II: Comparison with Visual Pill Ratings," *J. Text. Inst.*, vol. 89, no. 1, pp. 96–105, 1998.

[28] M. Eldessouki, H. A. Bukhari, M. Hassan, and K. Qashqari, "Integrated Computer Vision and Soft Computing System For Classifying The Pilling Resistance of Knitted Fabrics," *(In Press. FIBERS Text. East. Eur.*, vol. 22, no. 6(108), pp. 106–112, 2014.

[29] J. S. Weszka, C. R. Dyer, and A. Rosenfeld, "A Comparative Study of Texture Measures for Terrain Classification," *IEEE Trans. Syst. Man. Cybern.*, vol. SMC-6, 1976.

[30] R. M. Haralick, K. Shanmugam, and I. Dinstein, "Textural Features for Image Classification," *IEEE Trans. Syst. Man. Cybern.*, vol. 3, 1973.

[31] J.-S. R. Jang, "ANFIS: adaptive-network-based fuzzy inference system," *IEEE Trans. Syst. Man. Cybern.*, vol. 23, 1993.

[32] J. R. Jang, "Self-learning fuzzy controllers based on temporal backpropagation.," *IEEE Trans. Neural Netw.*, vol. 3, pp. 714–723, 1992.

Expert Systems with Applications 42 (2015) 2098–2113

Contents lists available at ScienceDirect

Expert Systems with Applications

journal homepage: www.elsevier.com/locate/eswa

Adaptive neuro-fuzzy system for quantitative evaluation of woven fabrics' pilling resistance

Mohamed Eldessouki [a,c,*], Mounir Hassan [b,c,1]

[a] Department of Materials Engineering, Technical University of Liberec, Czech Republic
[b] Faculty of Computing and Information Technology, King Abdulaziz University, Jeddah, Saudi Arabia
[c] Department of Textile Engineering, Faculty of Engineering, Mansoura University, Mansoura, Egypt

ARTICLE INFO

Article history:
Available online 22 October 2014

Keywords:
Adaptive neuro-fuzzy system
Quantitative evaluation
Textural features
Woven fabric pilling

ABSTRACT

Fabric pilling is considered a performance and aesthetic property of the woven products that determine its quality. The subjective evaluation of the fabric pilling results in misleading values that depend on the measurement standard even for the same sample. This work utilizes some textural features extracted from the fabric's images to obtain better representative and quantitative values of the fabric's surface. An algorithm for creating features dataset for training and testing the soft-computing classifier was described where random noise was added to the limited number of fabric's pilling standard images. The objective pilling classification of the fabric samples was performed using an adaptive neuro-fuzzy system (ANFIS) which showed an ability to classify the noised standard images with a correct classification rate of 85.8%. The ANFIS was also able to classify actual fabric samples with a Spearman's coefficient of rank correlation at +0.985 when compared with the classification grades of the human operators. Results showed high efficiency of the system that is independent on the different fabric structure or color which suggests its availability to replace the currently applied subjective pilling evaluation.

1. Introduction

The quality control of the textile products is one of the major factors that determine the price, and therefore the profit, of these products. Among the important properties of fabrics are the *performance properties* which represent the response of the fabric to a certain force, exposure, or treatment. Performance properties of a fabric include the fabric strength, abrasion resistance, pilling, and color fastness. Fabric pilling is one of those properties that can be classified as performance or aesthetic properties of the fabric and, therefore, being critical phenomena for both the manufacturers and the consumers. According to the ASTM standard terminology related to textiles (Committee, 2003), pills can be defined as "bunches or balls of tangled fibers which are held to the surface of a fabric by one or more fibers". The fabric pilling is affected by a wide range of parameters that may be related to: yarn parameters (e.g. twist, hairiness…, etc), spinning technology (e.g. ring spinning, rotor, compact spinning…, etc), fabric producing technology (e.g. weaving, knitting…, etc), as well as other processing parameters (Paek, 1989).

Evaluating the fabric pilling during the quality control process depends in the majority of standard testing methods on accelerated fabric wear using laboratory devices that simulate the frictional mechanisms lead to surface wear and pilling formation. The available standards recommend comparing samples that gone under this accelerated wear process with standard photographs of different pilling grades where expert operators can judge the samples and assign a pilling grade to them. This results in a subjective evaluation of the fabric pilling with a great dependency on the human element. The majority of pilling standard evaluation methods assign a ranking system that ranges between 1 and 5 (where 1 is assigned to a sever pilling and 5 is assigned to no pilling). However, the existence of different standards (e.g. ASTM, SN, EN ISO…, etc) creates a lot of confusion as the same sample may be ranked with different pilling grades according to the standard that was used in the evaluation. This calls researchers for finding alternative objective evaluation methods that may help to standardize those standard methods (Behera & Mohan, 2005).

Image analysis is a common technique in detecting textile faults (Eldessouki, Hassan, Qashqary, & Shady, 2014) including their esthetic character as well as their irregularities (Eldessouki, Ibrahim, & Militky, 2014). The introduction of image analysis as a method for evaluating the fabric pilling started in the late 80s as a try to replace the applied subjective evaluation methods (Konda, Xin, Okoshi, & Toriumi, 1988). The application of the image processing and analysis in the evaluation of fabric pilling goes through four main stages as indicated in Fig. 1 and the majority of the available literature on the topic tried to focus on one or more of these stages to modify the total outcome.

The main four objective pilling evaluation stages can be explained as follow:

1.1. Fabric's surface digitization

The fabric surface digitization is the process of converting the fabric surface to a digital form that can be dealt with on computer systems. This process can be done using a digital scanner (Kim & Kang, 2005; Palmer, Joud, & Wang, 2005; Palmer & Wang, 2003; Semnani & Ghayoor, 2009; Yun, Kim, & Park, 2013), a camera (Behera & Mohan, 2005; Hsi, Bresee, & Annis, 1998a; Torres & Navarro, 1998; Xin, Hu, & Yan, 2002), a light projected on camera (Chen & Huang, 2004), a camera attached to a microscope (Izabela, 2009), optical triangulation topographic reconstruction of the fabric surface (De Oliveira Mendes, Fiadeiro, & Miguel, 2010, 2011; De Oliveira Mendes, Fiadeiro, Miguel, & Lucas, 2009), a laser line projected on the surface of the fabric specimen (Kang, Cho, & Kim, 2004), or a stereovision surface reconstruction using two CCD cameras (Kang et al., 2004).

1.2. Pills detection and segmentation

Pills detection and segmentation is the process of separating the surface fuzz and pills from the complicated fabric structure background. This process was obtained using simple techniques such as the application of a binarization threshold on the fabric images (Kang et al., 2004; Konda et al., 1988), or after processing the raw fabric images using spatial and spectral techniques. The raw image processing may include some filters for noise reduction or edge detection (Semnani & Ghayoor, 2009), a background dilation and erosion (de Oliveira Mendes et al., 2009; Torres & Navarro, 1998), a fabric pattern detection and isolation using Fast Fourier Transform (FFT) (Behera & Mohan, 2005; Palmer, Zhang, & Wang, 2009; Torres & Navarro, 1998; Xin et al., 2002; Yun et al., 2013) or the different techniques of wavelet transforms (Palmer & Wang, 2003; Palmer et al., 2005, 2009; Zhang, Wang, & Palmer, 2007a, 2007b; Zhang, Wang, & Palmer, 2010). The pill detection was also performed using a template matching algorithm (Xin et al., 2002) and edge flow detection (Xiaojun, 2009; Xiao & Yang, 2007). For the colored images, pills were detected manually by blending the color channels of the fabric image (Izabela, 2009).

1.3. Pills quantization

The pills quantization is the next stage after segmenting pills from the fabric image. The process focuses on extracting some features that numerically represent the pills population to allow a quantitative discrimination between the different images. The feature descriptors can be divided in two categories; one that depends on the final image of the segmented pills, and the second that utilizes the spectral decomposition and analysis that was performed during the pills segmentation. The first category of features includes simple features such as the number of pills, the total pixel area of pilling, mean area of pills, the relative area of the pills to the total surface area, the sum of the gray values of pill images, the total volume of pills, as well as the distributions of pills, their shape, orientation angle, contrast, and density or uniformity of pills spatial distribution on the fabric surface (Behera & Mohan, 2005; de Oliveira Mendes et al., 2009; Hsi, Bresee, & Annis, 1998b; Izabela, 2009; Kang et al., 2004; Kim & Kang, 2005; Konda et al., 1988; Torres & Navarro, 1998; Xin et al., 2002; Yun et al., 2013). The descriptor features can also be calculated from the gray-scale image of the processed surface or from the simulated fabric surface and includes roughness, skewness, as well as pills number, volume (total and average volumes), height (maximum and average), area (total and average), and fractal dimension (Chen & Huang, 2004; Semnani & Ghayoor, 2009).

The second category of features includes the wavelet detail coefficients from the decomposition levels at the horizontal, the vertical and the diagonal orientations (Zhang et al., 2007a). It can be defined also as the horizontal detailed coefficient (especially at scale close to the inter-yarn distances in the fabric) (Palmer & Wang, 2003), as well as the energies of the reconstructed sub-images indifferent spatial orientations (Zhang et al., 2007b, 2010). Other statistical features can also be extracted from the wavelet decompositions such as the range, the inter-quartile range, the variance, the standard deviation, the mean absolute deviation, the median absolute deviation, the standard error and the coefficient of variation (Palmer et al., 2005).

1.4. Pills rating and classification

The classification stage is the ultimate goal of the whole process where a "successful" rating of images allows the trust in the method to replace the available subjective analysis. Classification models use the extracted set of features as inputs that can be used to generate the final rating of the image. The classification models may implement empirical and statistical methods such as the multi-variable linear regression (Kang et al., 2004; Kim & Kang, 2005; Xin et al., 2002) and discriminant analysis (Palmer et al., 2005; Zhang et al., 2007a, 2007b),or may implement artificial intelligent methods such as the application of different types of the artificial neural networks (Chen & Huang, 2004; Eldessouki et al., 2014; Zhang et al., 2010).

Based on this literature survey, three points can be highlighted:

- Although fabric wear and pilling are affecting the *texture* of the surface, there is no available publication that considers the image "textural parameters" during the pilling quantization.
- The classification methods based on artificial intelligence techniques require big databases for the system training and verification. However, the size of the dataset is limited because this dataset is based on photographs that are taken from standard images. Since the majority of standard methods utilize a rating system from 1 to 5, the standard images have a limited number that is not enough for creating a reasonable dataset size.
- There are few papers that consider the efficient techniques of each evaluation stage to create an integrated, robust, and effective evaluation process. On the other hand, the majority of these papers focus on enhancing one or more of these stages separately.

Therefore, this work tries to address these problems by:

- Considering the *texture features* of the images among the quantization parameters.
- Introducing a new method for creating sampling dataset that is large enough to suite the training and testing processes required in building the applied artificial intelligent classifier.

Fig. 1. Stages of quantitative fabric pilling evaluation.

- Utilizing the neuro-fuzzy classification system to approach the high level of evaluation in human beings.
- Creating a user-friendly system that integrates the four evaluation stages. The system is semi-automatic in a way that classifies the pilling in the introduced sample automatically and allows the operator to change some of the detection parameters if not satisfied with the automatic detection.

2. Computation theory

2.1. Image preparation

The EMPA Standard (SN 198525) was used to obtain the standard images for pilling ranking. The EMPA standard has two series of photographs; the *K*-series for the knitted fabrics and the W-series for the woven fabrics. Among the W-series, there is the W1 category for evaluating the nonwoven fabrics while the W2 and W3 categories are used for evaluating the woven fabrics (Behera & Mohan, 2005). The W2 category is usually used in evaluating samples with big pill size while W3 is more suitable with samples of smaller pills. Within each category, there are four standard pictures used in the comparison and pills ranking on a scale of 1 (for the worst) to 5 (for the pill-free). To help the operators with their "fuzzy" and "subjective" evaluation, there are only four pictures for the five ranks where the first picture represents ranks 1-to-2, the second picture represents ranks 2-to-3, …, etc. The standard photographs were scanned to the computer with a resolution of 600 × 600 dpi.

To generate a dataset with a suitable size out of these limited standard pictures, each standard image was duplicated many times where each copy had a random noise that was applied to it. To add noise to the pictures, different filter kernels were created with random parameters and each filter was convoluted with the picture to create a "noised" or "blurred" image. The applied filters are the "averaging", "disk", "Gaussian", "motion" filters, and the "partial spatial rearrangement". Representation of the original image and samples after the application of different noise filters are shown in Fig. 2. The kernel for each filter was generated using random parameters that change each time of recalling the filter. The "partial spatial rearrangement" technique was applied by randomly selecting sub-image from the pilling region of the sample and having a size that represents 10% of the original image then placing the sub-image in a random way at a different position of the image.

These five types of noise generators were applied three times using random parameters to each standard picture which creates 15 noised copies of the original image. To avoid the system bias to the noised images, the features extracted from the original image were duplicated 35 times to create a features dataset with 30% representation of the noised images. The features dataset consists of the previously mentioned 4 features with 200 observations (50 observations for each standard image) of each standard category (W1, W2, and W3). The features dataset was then split randomly into a training dataset that represents 80% and a testing dataset that represents the remaining 20% of the data. The introduction of the noised images during the training of the classification system makes it more robust to classify different samples even with noised pictures.

2.2. Textural features

The basic statistics that are utilized in pilling quantization (the first order statistical features) extract data out of the gray-scale levels of the pixels in the digital image and does not reflect these surface features. On the other hand, the second order and textural features are more concerned about the spatial distribution of the gray-scale levels which reflects the roughness of the image and its texture. This gives the advantage of being close to the human awareness of the texture that describe surfaces as fine, coarse, smooth, rippled, irregular,… etc.

For an image with *x* and *y* representing the spatial coordinates, the gray-scale levels of that image can be expressed as $\boldsymbol{P}(x,y)$ and its gray level co-occurrence matrix (GLCM) can be calculated to determine the textural features of the image. The GLCM represents the joint probability density of the pairs of the gray levels occur at pairs of points separated by the vector $\delta(\Delta x,\Delta y)$ (Weszka, Dyer, & Rosenfeld, 1976). The displacements Δx and Δy in the vector δ determine the length (the running distance d) and the angel (direction θ) between the points of the required calculation. The calculated joint density takes the matrix form $\boldsymbol{C_\delta}$ with a size $N\delta N$ where N is the maximum value of gray levels in the original image $\boldsymbol{P}$ and the value $\boldsymbol{C_\delta}(i,j)$ represents the probability of the pair of gray levels (i,j) occurring at separation δ. To illustrate the calculation of the GLCM, consider the example shown in Fig. 3 for an image $\boldsymbol{P}(x,y)$ with $N = 4$ gray levels values that range between 0 and 3. Therefore, the size of the co-occurrence matrix $\boldsymbol{C}$ is 4×4 and for a separation vector $\delta(1,0)$ the entries $\boldsymbol{C_\delta}(i,j)$ are the number of times gray level i occur immediately (*i.e.* one pixel distance) to the left (*i.e.* in zero angel direction) of the gray level j.

Once the co-occurrence matrix was calculated the image texture can be analyzed based on the given parameters (d,θ) of the vector δ. If the image's texture is coarse and the displacement d is smaller than the size of the texture element, the pairs of points at separation δ should have similar gray levels. Therefore, the high values in the co-occurrence matrix $\boldsymbol{C_\delta}$ should be concentrated at the main diagonal or its nearby. Similarly, for fine textured images with texture elements comparable in size to the separation δ, the values in $\boldsymbol{C_\delta}$ will be spread out. The same logic applies for the texture direction that might be directed to a certain angel and, therefore, the spread of the values about the main diagonal of $\boldsymbol{C_\delta}$ will depend on the selected angel (θ) of the vector δ. Therefore, an investigation of the image texture is required at different displacements (d) and directions (θ) then the scattering of values around the $\boldsymbol{C_\delta}$'s main diagonal should be measured.

To measure the spread of values in the co-occurrence matrix Haralick, Shanmugam, and Dinstein (1973) suggested different features that represent the texture information of the image. The calculation of these features starts usually with the normalization of the matrix $\boldsymbol{C}$ by its total sum:

$$D_\delta(i,j) = \frac{\boldsymbol{C}_\delta(i,j)}{\sum_{i,j=0}^{N-1}\sum_{i,j=0}^{N-1}\boldsymbol{C}_\delta(k,l)}$$

where i, j, k, and l are indices and $\boldsymbol{D}_\delta$ is the normalized matrix at a certain direction δ.

Among the features suggested by Haralick, four features were found to be more effective and will be tested in this study. These features are:

Contrast:

$$f_{1,\delta} = \sum_{i=1}^{N}\sum_{j=1}^{N}(i-j)^2 D_\delta(i,j)$$

The contrast is also known as the "*variance*", and the "*inertia*" and it is taken as a texture feature because it represents the moment of inertia of the matrix $\boldsymbol{D}_\delta$ around its main diagonal and it is a measure of the degree of its spread of values.

Correlation:

$$f_{2,\delta} = \sum_{i=1}^{N}\sum_{j=1}^{N}\frac{ijD_\delta(i,j)-\mu_i\mu_j}{\sigma_i\sigma_j}$$

where μ_i and σ_i are the mean and standard deviation, respectively, of the row sums and μ_j, and σ_j are the mean and standard deviation, respectively, of the column sums of the matrix $\boldsymbol{D}_\delta$. The correlation is a measure of the degree to which the rows (or columns) of the GLCM resemble each other and this value should be high when values are uniformly distributed in the matrix and low when the values off the diagonal are small.

Angular second moment (ASM):

$$f_{3,\delta} = \sum_{i=1}^{N}\sum_{j=1}^{N}D_\delta(i,j)^2$$

The angular second moment (ASM) is also known with different names such as the "*energy*", the "*uniformity*", and the "*uniformity of energy*". This value is small when $\boldsymbol{D}_\delta(i,j)$ are close in values and it increases when values largely varied as in the situation where values are clustered near the main diagonal.

Inverse difference moment (IDM):

$$f_{4,\delta} = \sum_{i=1}^{N}\sum_{j=1}^{N}\frac{D_\delta(i,j)}{1+(i-j)^2}$$

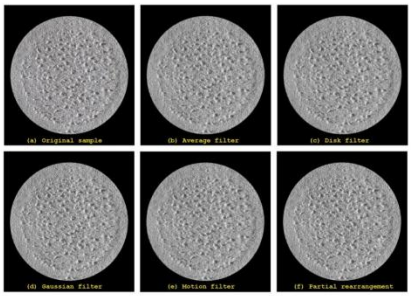

Fig. 2. Examples for different shapes of the same fabric sample after applying random filters.

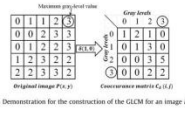

Fig. 3. Demonstration for the construction of the GLCM for an image $P(x,y)$.

The inverse difference moment (IDM) can also be called the *homogeneity* and it measures the closeness of the distribution of elements in the GLCM to its diagonal and it reaches 1 for a diagonal matrix.

2.3. Adaptive neuro-fuzzy system

Fuzzy inference systems are useful in mapping data between two spaces while some degree of uncertainty is involved. The fuzzy system implements the membership functions, instead of the crisp-set functions, to imitate the human thinking and cognition without employing precise quantitative analyses (Jang, 1993). This provides the opportunity to deal with imprecision and to represent the linguistic qualitative words such as "many", "low", "few"…, etc. However, creating such fuzzy systems requires some understanding of the rules that govern the relations between the inputs and the outputs. Therefore, the adaptive neuro-fuzzy inference systems (ANFIS) were introduced to combine the natural language description of fuzzy systems and the learning properties of neural-networks. By using a hybrid learning algorithm, the ANFIS can construct an input–output mapping based on both human knowledge (in the form of fuzzy *if–then* rules) and stipulated input–output data pairs (Jang, 1993).

The initial model of the ANFIS was proposed by Jang (1992, 1993) who explained it using two inputs (x_1, x_2) and built the rule based system using two *if-then* rules, although the system can be generalized to any *N* number of inputs or *M* rules. The model with two inputs is demonstrated in Fig. 4 with five layers that include two *adaptive* layers (layer #1 and layer #4, demonstrated by rectangles) and three *fixed* layers (layer #2, layer #3, and layer #5, demonstrated by circles). The two adaptive layers are distributed between the *premise* part, and the *consequent* part which are the two basic components of all *logical statements*. The positioning of

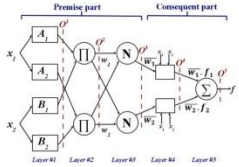

Fig. 4. The ANFIS model.

the adaptive layers at these two parts allows the adjustment of their parameters and consequently adjusting the performance of the whole system.

The two rules of Takagi and Sugeno were applied as:

Rule 1: If x_1 is A_1 and x_2 is B_1, then $f_1 = p_1x_1 + q_1x_2 + r_1$.
Rule 2: If x_1 is A_2 and x_2 is B_2, then $f_2 = p_2x_1 + q_2x_2 + r_2$

The output of the kth layer can be expressed with the vector O^k which can be stated for the first layer O^1 in the form:

$$O_i^1 = \begin{cases} \mu_{A_i}(x_1) \\ \mu_{B_i}(x_2) \end{cases}$$

where μ_{A_i} and μ_{B_i} are the membership functions (MF) for the first and the second inputs, respectively. The membership function can take different shapes of any continuous and piecewise differentiable functions. The selected MF in this case is the Gaussian (bell shape) function with normalized output ϵ [0, 1] which can be written for the first input (x_1) in the following form (and a similar relation can be found for the second input):

$$\mu_{A_i}(x_1) = e^{-\left(\frac{x_1 - a_i}{b_i}\right)^2}$$

where; the parameters {a_i and b_i} determine the shape and behavior of the membership function. These parameters will be called the *premise parameters* as they are the adjustable parameters in the premise part.

The neuron elements of the second layer are fixed with simple multiplication transfer function. The output of each neuron represents the *firing strength* of the rule. The output vector of this layer (O^2) can be calculated as:

$$O_i^2 = w_i = \mu_{A_i}(x_1) \cdot \mu_{B_i}(x_2)$$

The third layer is a fixed layer with the role of normalizing its inputs to produce the *normalized firing strength* which is the ratio of the firing strength of the ith rule to the sum of the firing strength for all rules, that is:

$$O_i^3 = \overline{w}_i = \frac{w_i}{\sum_{i=1}^{N} w_i} = \frac{w_i}{w_1 + w_2}$$

where, N is the number of the system inputs.

The fourth layer is the adaptive layer that multiplies the normalized firing strength by a first order polynomial for the first order Takagi and Sugeno model. The output vector of this layer O^4 can be expressed as:

$$O_i^4 = \overline{w}_i f_i = \overline{w}_i(p_i x_1 + q_i x_2 + r_i)$$

where, the parameters {p_i, q_i, and r_i} are adjustable and can be used to tune the outputs of that layer. These parameters will be called the *consequent parameters* as they tune the output of the consequent part of the system.

The fifth layer has a single fixed neuron that sums up its inputs and produces the final result (f) of the system that can be represented as:

$$O_i^5 = f = \sum_{i=1}^{N} \overline{w}_i f_i = \frac{\sum_{i=1}^{N} w_i f_i}{\sum_{i=1}^{N} w_i}$$

2.4. Hybrid learning algorithm for the ANFIS

The goal of the learning of the ANFIS is to adjust all the tunable system parameters which includes both the premise parameters (a_i and b_i) and the consequent parameters (p_i, q_i, and r_i) to minimize the overall system's error. The hybrid learning algorithm utilizes two passes: the forward pass with fixed premise parameters and the backward pass with fixed consequent parameters. To explain that, consider the forward pass with fixed premise

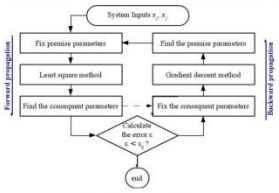

Fig. 5. Hybrid ANFIS learning algorithm.

Table 1
Tested knitted sample specifications.

	Color	Structure	Weight/area (g/m²)	Warp density (threads/inch)	Weft density (threads/inch)	Warp count (tex)	Weft count (tex)
W1	White	1/6	128	71	70	21	21
W2	White	1/1	155	63	60	30	31
W3	Bright white	1/1	121	81	51	19	26
W4	Blue	1/3	145	86	56	21	32
W5	Blue	2/4	157	87	64	22	29
W6	Light blue	1/3	167	88	55	21	38
W7	Paige	1/2	182	89	79	24	25

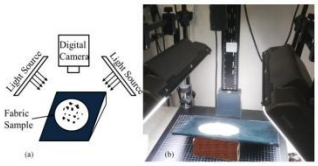

Fig. 6. Image acquisition setup depicted schematically in (a) and photographed in (b).

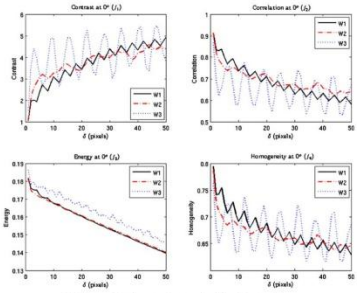

Fig. 7. Features of the three categories at an angle of 0° and short term distance.

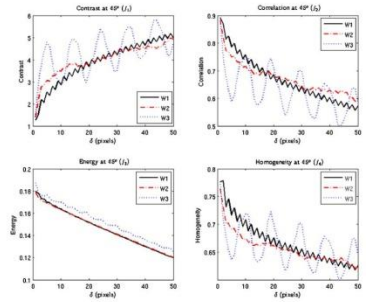

Fig. 8. Features of the three categories at an angle of 45° and short term distance.

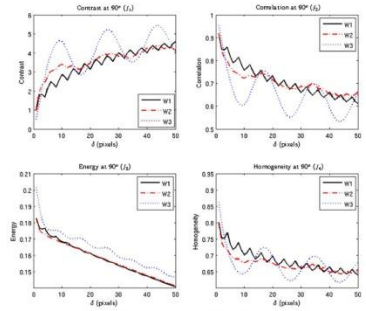

Fig. 9. Features of the three categories at an angle of 90° and short term distance.

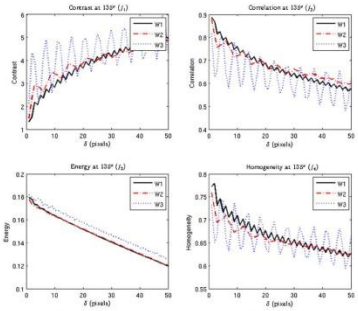

Fig. 10. Features of the three categories at an angle of 135° and short term distance.

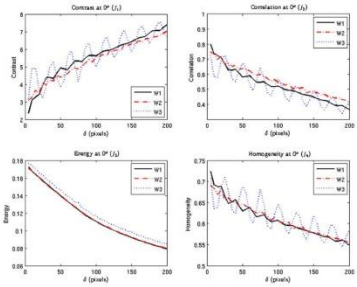

Fig. 11. Features of the three categories at an angle of 0° and long term distance.

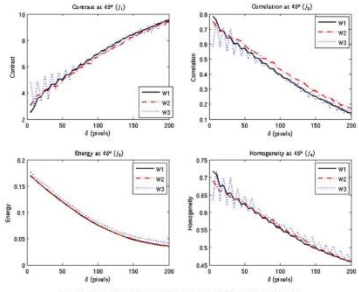

Fig. 12. Features of the three categories at an angle of 45° and long term distance.

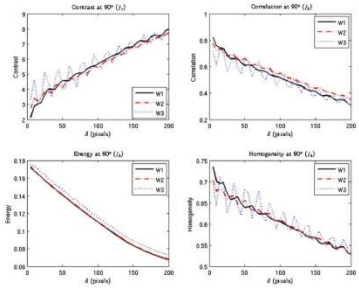

Fig. 13. Features of the three categories at an angle of 90° and long term distance.

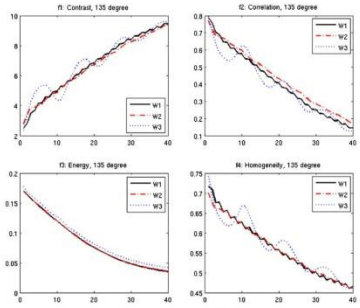

Fig. 14. Features of the three categories at an angle of 135° and long term distance.

Table 2
Features periodicity at short distance (values in pixels).

		f_1	f_2	f_3	f_4
Zero	W1	4	4	–	4
	W2	9	–	–	9
	W3	6.5	6.5	–	6
45°	W1	4	4	–	4
	W2	9	9	–	9
	W3	6	6	–	6
90°	W1	4	4	–	4
	W2	15	15*	–	9
	W3	17	17	–	17
135°	W1	2	2	–	2
	W2	6.5	6.5	–	7
	W3	5	5	–	5

* Low correlation was observed at these values.

parameters which results in an output that can be defined for the given two inputs ANFIS as:

$$f = \overline{W_1} f_1 + \overline{W_1} f_1 = \overline{W_1}(p_1 x_1 + q_1 x_2 + r_1) + \overline{W_2}(p_2 x_1 + q_2 x_2 + r_2)$$

That can be rearranged to:

$$f = (\overline{W_1} x_1) p_1 + (\overline{W_1} x_2) q_1 + (\overline{W_1}) r_1 + (\overline{W_2} x_1) p_2 + (\overline{W_2} x_2) q_2 + (\overline{W_2}) r_2$$

It can be noticed from this equation that it represents a linear combination of the consequent parameters $\{p_1, q_1, r_1, p_2, q_2,$ and $r_2\}$. The least square method can be utilized to calculate those parameters. Therefore, the signal goes in the forward pass along the system until layer #4 then the least square method can be applied to allocate the consequent parameters and the whole system can be identified. The error rate of the system can be calculated after the system identification. The backward pass starts with fixing the consequent parameters and propagating the error rate backward through the system and the premise parameters $\{a_i$ and $b_i\}$ can be updated by the gradient descent method. This cycle continues until the desired performance is achieved as illustrated in Fig. 5.

3. Experimental setup

Seven woven fabrics with different structures and colors are used and the specifications of these samples are listed in Table 1. To test the system ability in detecting the fabric pilling regardless of the color shade, the tested samples were selected to have different colors. Samples were tested on Martindale instrument for pilling where two circular specimens of 140 mm diameters

Table 3
Features periodicity at long distance (values in pixels).

		f_1	f_2	f_3	f_4
Zero	W1	20	20	–	20
	W2	10	10	–	10
	W3	25	25	–	25
45°	W1	–	10	–	10
	W2	–	25	–	25
	W3	10	10	–	10
90°	W1	20	20	–	20
	W2	15	15	–	15
	W3	20	20	–	20
135°	W1	10	10	–	10
	W2	–	–	–	–
	W3	55	55	–	55

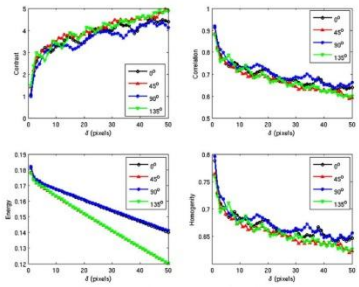

Fig. 15. Features as calculated at different angles for sample W2_1-2.

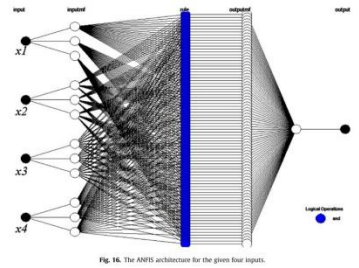

Fig. 16. The ANFIS architecture for the given four inputs.

from each sample were placed on the machine head. The face of the lower specimen is up and the specimen is placed on the top of a standard felt of 140 mm diameter. The upper specimen is mounted on a holder of 90 mm diameter with a standard felt of the same size and fixed to the holder with an elastic ring. The upper holder is installed on the machine where the faces of the upper and lower specimens are in contact to each other. The samples were tested under 6.5 cN/cm^2 pressure for 10,000 cycles of Lissajous figure with 24 mm stroke.

The measured samples were evaluated visually by seven different operators against the photographs of the EMPA Standards (SN 198525). The measured samples were then digitized using

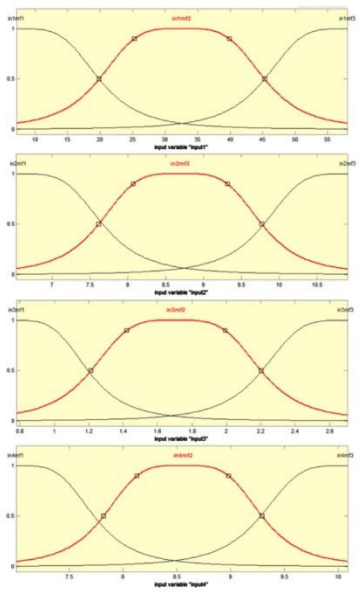

Fig. 17. The adjusted membership functions for the four inputs (each input has two MFs).

the setup shown in Fig. 6 and processed using the developed software algorithm to obtain the pilling classes. The image acquisition system consists of a digital CCD camera that is equipped with a macro lenses to capture the sample surface details. The captured image resolution of 300 dpi and the image dimensions was 2048 × 1536 pixels. Lighting is critical for the imaging system and two light sources that equally distribute the light on the surface of the fabric were applied. The sample was tilted with a slight angel to the horizontal plane to allow contrasting the pills with their shadow.

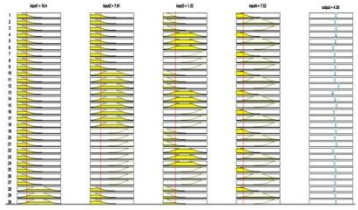

Fig. 18. The application of the ANFIS.

4. Results and discussion

Pre-investigation for the effective choice of the vector δ was performed by applying a distance sweep in the range of $d = 0$ to 50 with a step of one pixel. For long range investigations, another distance sweep in the range of 5 to 200 with a step of 5 pixels was also performed. In each case of the evaluation (the short term and the long term), a direction sweep was performed at four angles $\theta = 0°$, 45°, 90°, and 135°. Results of the four extracted features for the short and long term distance sweeps are shown in Figs. 7–14 for the first sample of each standard category (i.e. W1_1-2, W2_1-2, and W3_1-2).

From these figures some general notes can be observed on the fabric surface and its textural features:

- The behavior of the contrast feature (f_1) increases with increasing the calculation distance (δ) which is different from the other three features that decrease with distance.

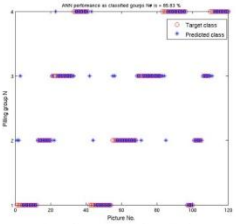

Fig. 19. Performance of the ANFIS for the Nth grade.

- There is a form of periodicity in the behavior of most features, although this periodicity is not dominant in the energy feature (f_3) compared to the other features.
- The periodicity of the features can be considered as an indicator of the repeatability of objects on the fabric's surface at a certain distance. For example, by examining features f_1, f_2, f_3, f_4 at an angle of zero in Fig. 7, a cyclic pattern can be observed with repeats of 4 pixels in category W1, 9 pixels in category W2, and 6 pixels in category W3. This indicates a repeatability of objects at these distances which might imply the repeatable pattern of the woven structure.
- The periodicity of features shown in Figs. 7–10 at short distances is summarized in Table 2 while the periodicity of the long distances shown in Figs. 11–14 is summarized in Table 3. Some features show periodicity although it might not be strong in some cases which were highlighted in the table with "low" and with the periodic interval, when available.
- Periodicity interval is almost constant when obtained from different features for the same fabric image.
- There is a small effect of the calculation angle on the periodicity of the features where similar intervals can be observed at different angles. The cases where a difference can be observed for the feature at different angles (e.g. f_1 at the angles 0° and 90°) might be attributed to the different warp and weft densities in the image.
- The repeat for a feature as observed at long distances is a multiplier of the repeat value for the same feature at short distance. For example the repeat of f_1 at 0° for W1 is 4 pixels (Table 2) while this value is 20 pixels (Table 3) when measured at long distance. This can be attributed to the different step size of evaluation during the short distance (1 pixel) and the long distance (5 pixels).
- Features that repeat at short distances were found to diminish after certain distance. For instance, the feature f_1 at 45° for W3 is found to have a strong repeating wave as observed in Fig. 8 while this wave diminishes at long distances as shown in Fig. 12. This indicates the lack of correlation between the textural objects on the fabric's surface at long distances.

On the other hand, the change of the features at different directions at short distances is shown in Fig. 15. There is a high similarity of the features' general trend at different angles with a coincidence allocation of the peaks at certain distances. The

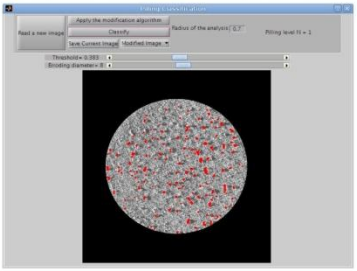

Fig. 20. GUI of the developed software for fabric's pilling evaluation.

strength of the repeatable peak is decaying with distance and there is no significant repeatable behavior observed at longer distances (up to 200 pixels). The frequency of the peaks at 90° is almost double the frequency at 0° while a similar high frequency can be found at the angles 45° and 135°.

According to this pre-investigation, the actual samples are evaluated at an angle of 45° which should be a reasonable step that will coincide with angles of 0°, 90°, and 135° as indicated in the previously discussed figure. Features are also evaluated at a range of distance that covers the periods of peak maxima of the different features of the three categories. Based on the repeatability values listed in Table 2, the features are calculated in the distance interval from 4 to 10 pixels then values are summed up to be used as the characteristic features of the image during its evaluation. Also, due to the behavior similarity for the features, only the contrast and the correlation are used during the evaluation. These features are selected because they have a repeatable behavior and opposite trends. The other two features for evaluating the fabric pilling will be the number of pills and their relative area which is calculated as ratio between the pills area and the total area of interest in the studied sample.

Based on the described algorithm, an adaptive neuro-fuzzy system was constructed as shown in Fig. 16 where the first adaptive layer consists of 3 neurons (3 membership functions) for each input. The premise parameters of this layer were calculated and the adjusted membership functions for the four inputs are shown in Fig. 17. The multiplication and normalization were performed in the rule layer which is highlighted in Fig. 16 with the blue color. The second adaptive layer is also shown in the same figure where the Takagi and Sugeno model applies and the consequent parameters are evaluated.

The application of the ANFIS system is demonstrated in Fig. 18 which includes the five basic steps of the calculation. The system starts with the *fuzzification* of the inputs where each input is processed in parallel through the membership functions. Second, the rules are applied using the *fuzzy operator* (AND) which results in the weighted firing strength to the third part of the *implication* and transfers data from the premise to the consequent. The fourth step is defined by the *aggregation* of the consequents across the rules and the final step is the *defuzzification* of the results to produce the final output.

The given ANFIS structure was trained with the contrast, correlation, number of pills, and their relative areas as inputs and the standard pilling grades or ranks (1, 2, 3, 4 or 5) as outputs. The performance of the ANFIS systems is shown in Fig. 19. For the 120 samples presented to the ANFIS systems, it can be seen that the ANFIS performed 85.8% in determining the pilling grade. Also, from these figures it can be observed that most of the samples that were

Table 4
Human operators as compared to the ANFIS pilling evaluation.

	OP.#1	OP.#2	OP.#3	OP.#4	OP.#5	OP.#6	OP.#7	Operators' evaluation	ANFIS evaluation
W1	3	3	1	2	2	2	2	2	2
W2	4	4	4	4	4	3	4	4	4
W3	3	2	2	1	4	2	2	2	2
W4	2	3	2	3	3	1	2	2	3
W5	2	1	1	1	3	2	1	1	1
W6	4	5	4	4	4	5	4	4	4
W7	3	3	3	3	4	2	5	3	3

miss-graded were deviated from the target class with only one degree which is acceptable in classifying such samples where the standards give two grades in the same picture.

Although the relatively high performance of the ANFIS in detecting the correct pilling of the noised standard images, it is important to test the system on real fabric samples. Therefore, the developed algorithm was coded in a user-friendly graphical user interface (GUI) that is shown in Fig. 20. The woven samples were introduced to seven human operators after their pilling test on Martindale to compare the samples with the standard pictures. The operators subjectively assigned a pilling rank for each sample as shown in Table 4 and the total pilling evaluation of the sample was calculated by the mode of the operator's ranks. The pictures of the woven samples were also introduced to the developed program that utilizes the ANFIS to rank the samples. The samples' pilling rank is listed in Table 4 and the Spearman's coefficient of rank correlation between the two categories of the human evaluation and the ANFIS evaluation is +0.982 which implies a good agreement between the two sets of results and a reliability of the system to be used in replacing the subjective evaluation of human operators.

5. Conclusion

This work introduces for the first time, to the best of the authors' knowledge, fabric's *image textural features* as measures for the fabric surface during the quantitative evaluation of pilling in woven fabrics. Creating a feature dataset from the available Standard images with enough size for training soft computing algorithms is challenging due to the limited number of those Standard images. To deal with this issue, a new approach was suggested to mimic the noise that interferes with the fabric surface during its digitization. Hence, a user-friendly pilling evaluation system that integrates the processes of fabric surface digitization, pilling segmentation, quantization, and classification was implemented in this work. The system was able to classify woven fabric samples according to their surface texture with a high degree of correlation to the traditional methods of pilling evaluation.

Results of textural features show a trend similarity between the features which allows the reduction of the number of these features during the evaluation (contrast and correlation were only used in the final code); Selection of few features was not only to prevent redundancy in the system's inputs, but also to allow other pilling descriptors (such as the number of pills and their relative area) that represent pilling intensity to be considered. Taking more pilling descriptors into account during the pilling quantization might be useful; however the computational resources required for the ANFIS classifier increases exponentially with the increase in number of the system's inputs. This applies a constraint on the number of pilling descriptors that can be simultaneously used during the ANFIS classification which results in a "features optimization problem" due to the need of features that represent both the image texture as well as the pilling intensity quantifiers. A major part of the figures in the results section presented in this work was dedicated to investigate the *texture features* at different conditions and optimize their selection.

The application of random noise filters on the Standard images significantly affects the textural features while keeping a small effect on the pilling intensity features. The parameters of the applied filters were randomly selected; however the range of these parameters should extend to apply more "aggressive" noise to the pictures to allow the robustness of the system to deal with fabric images of different structures and textures. Also, more noise filters might be required to better resemble the image defects that might occur during the image acquisition, although the current filters were useful in increasing the amount of sampling datasets.

Success in digitizing the Standard samples in the same systematic fashion of real samples (rather than scanning Standard images) should increase the reliability of the suggested system and allows it to be standardized as a quantitative method that replaces the current subjective evaluation Standards. The relatively good results of the suggested system are promising for the methodology extension to cover fabrics that are produced using different technologies (knitted and nonwoven fabrics) as well as fabrics of different structures.

References

Behera, B. K., & Mohan, T. E. M. (2005). Objective measurement of pilling by image processing technique. *International Journal of Clothing Science and Technology, 17*(5), 279–291.

Chen, X., & Huang, X. B. (2004). Evaluating fabric pilling with light-projected image analysis. *Textile Research Journal, 74*(11), 977–983.

Committee, D. (2003). ASTM D123-13a standard terminology relating to textiles. ASTM. Retrieved from <http://www.astm.org/Standards/D123.htm>.

De Oliveira Mendes, A., Fiadeiro, P. T., & Miguel, R. A. L. (2010). Subjective and objective pilling evaluations of textile fabrics: A comparison. *Textile Research Journal, 80*(18), 1887–1897.

De Oliveira Mendes, A., Fiadeiro, P. T., & Miguel, R. A. L. (2011). Virtual subjective pilling evaluation: An alternative. *Textile Research Journal, 81*(9), 892–901.

De Oliveira Mendes, A., Fiadeiro, P. T., Miguel, R. A. L., & Lucas, J. M. (2009). Optical estimation of a set of pilling coefficients for textile fabrics. *Textile Research Journal, 79*(5), 410–417.

Eldessouki, M., Bukhari, H. A., Hassan, M., & Qashqari, K. (2014). Integrated computer vision and soft computing system for classifying the pilling resistance of knitted fabrics. *FIBRES & TEXTILES in Eastern Europe, 22*(6(108)), 106–112.

Eldessouki, M., Ibrahim, S., & Militky, J. (2014). A dynamic and robust image processing based method for measuring yarn diameter and its variation. *Textile Research Journal, 84*(18), 1948–1960. http://dx.doi.org/10.1177/0040517514538032.

Eldessouki, M., Hassan, M., Qashqary, K., & Shady, E. (2014). The application of principal component analysis to boost the performance of the automated fabric fault detector and classifier. *FIBRES & TEXTILES in Eastern Europe, 22*(4(106)), 51–57.

Haralick, R. M., Shanmugam, K., & Dinstein, I. (1973). Textural features for image classification. *IEEE Transactions on Systems, Man, and Cybernetics*, 3. http://dx.doi.org/10.1109/TSMC.1973.4309314.

Hsi, C. H., Breese, R. R., & Annis, P. A. (1998a). Characterizing fabric pilling by using image-analysis techniques. Part I: Pill detection and description. *Journal of the Textile Institute, 89*(1), 80–95.

Hsi, C. H., Breese, R. R., & Annis, P. A. (1998b). Characterizing fabric pilling by using image-analysis techniques. Part II: Comparison with visual pill ratings. *Journal of the Textile Institute, 89*(1), 96–105.

Izabela, J. (2009). Assessment of a fabric surface after the pilling process based on image analysis. *FIBRES & TEXTILES in Eastern Europe, 17*(2), 73.

Jang, J. R. (1992). Self-learning fuzzy controllers based on temporal backpropagation. *IEEE Transactions on Neural NetworksA Publication of the IEEE Neural Networks Council, 3*, 714–723. http://dx.doi.org/10.1109/72.159060.

Jang, J.-S. R. (1993). ANFIS: Adaptive-network-based fuzzy inference system. *IEEE Transactions on Systems, Man, and Cybernetics, 23*. http://dx.doi.org/10.1109/21.256541.

Kang, T. J., Cho, D. H., & Kim, S. M. (2004). Objective evaluation of fabric pilling using stereovision. *Textile Research Journal, 74*(11), 1013–1017.

Kim, S. C., & Kang, T. J. (2005). Image analysis of standard pilling photographs using wavelet reconstruction. *Textile Research Journal, 75*(12), 801–811.

Konda, A., Xin, L. C., Okoshi, Y., & Toriumi, K. (1988). Evaluation of pilling by means of computer image analysis. Part 2: Evaluation of pilling classes. *Sen'i Kikai Gakkaishi (Journal of the Textile Machinery Society of Japan), 41*(11), T152–T161.

Paek, S. L. (1989). Pilling, abrasion, and tensile properties of fabrics from open-end and ring spun yarns 1. *Textile Research Journal, 59*(10), 577–583.

Palmer, S. R., Joud, L., & Wang, X. (2005). Characterization and application of objective pilling classification to patterned fabrics. *Journal of the Textile Institute, 96*(6), 423–430.

Palmer, S., & Wang, X. (2003). Objective classification of fabric pilling based on the two-dimensional discrete wavelet transform. *Textile Research Journal, 73*(8), 713–720.

Palmer, S., Zhang, J., & Wang, X. (2008). New methods for objective evaluation of fabric pilling by frequency domain image processing. *Research Journal of Textile and Apparel, 12*(1), 11–23.

Semnani, D., & Ghayoor, H. (2009). Detecting and measuring fabric pills using digital image analysis. *World Academy of Science, Engineering and Technology, 49*, 897–900.

Torres, Y., & Navarro, R. (1998). Automatic method based on image analysis for pilling evaluation in fabrics. *Optical Engineering, 37*(11), 2937–2947.

Weszka, J. S., Dyer, C. R., & Rosenfeld, A. (1976). A comparative study of texture measures for terrain classification. *IEEE Transactions on Systems, Man, and Cybernetics, SMC-6*. http://dx.doi.org/10.1109/TSMC.1976.5408777.

Xiao, Z.-f., & Yang, H.-W. (2007). Fabric pilling segmentation based on edgeflow algorithm. *2007 International conference on machine learning and cybernetics* (Vol. 3, pp. 1744–1748). IEEE.

Xiaojun, L. (2009). Segmentation for Fabric Pilling Images Based on Edge Flow. *Second international conference on information and computing science, 2009. ICIC'09* (Vol. 2, pp. 369–372). IEEE.

Xin, B., Hu, J., & Yan, H. (2002). Objective evaluation of fabric pilling using image analysis techniques. *Textile Research Journal, 72*(12), 1057–1064.

Yun, S. Y., Kim, S., & Park, C. K. (2013). Development of an objective fabric pilling evaluation method. I. Characterization of pilling using image analysis. *Fibers and Polymers, 14*(5), 832–837.

Zhang, J., Wang, X., & Palmer, S. (2007a). Objective grading of fabric pilling with wavelet texture analysis. *Textile Research Journal, 77*(11), 871–879.

Zhang, J., Wang, X., & Palmer, S. (2007b). Objective pilling evaluation of wool fabrics. *Textile Research Journal, 77*(12), 929–936.

Zhang, J., Wang, X., & Palmer, S. (2010). Objective pilling evaluation of nonwoven fabrics. *Fibers and Polymers, 11*(1), 115–120.